

# STRUCTURE, COMPOSITION, PHYSICAL PROPERTIES, AND TURNOVER OF PROLIFERATED PEROXISOMES

## A Study of the Trophic Effects of Su-13437 on Rat Liver

FEDERICO LEIGHTON, LUCY COLOMA, and CECILIA KOENIG

From the Departamento de Biología Celular, Universidad Católica de Chile, Santiago, Chile. Dr. Leighton's present address is the International Institute of Cellular and Molecular Pathology, B-1200 Brussels, Belgium.

### ABSTRACT

Peroxisome proliferation has been induced with 2-methyl-2-(*p*-[1,2,3,4-tetrahydro-1-naphthyl]-phenoxy)-propionic acid (Su-13437). DNA, protein, cytochrome oxidase, glucose-6-phosphatase, and acid phosphatase concentrations remain almost constant. Peroxisomal enzyme activities change to approximately 165%, 50%, 30%, and 0% of the controls for catalase, urate oxidase, L- $\alpha$ -hydroxy acid oxidase, and D-amino acid oxidase, respectively. For catalase the change results from a decrease in particle-bound activity and a fivefold increase in soluble activity. The average diameter of peroxisome sections is  $0.58 \pm 0.15 \mu\text{m}$  in controls and  $0.73 \pm 0.25 \mu\text{m}$  after treatment. Therefore, the measured peroxisomal enzymes are highly diluted in proliferated particles.

After tissue fractionation, approximately one-half of the normal peroxisomes and all proliferated peroxisomes show matrix extraction with ghost formation, but no change in size. In homogenates submitted to mechanical stress, proliferated peroxisomes do not reveal increased fragility; unexpectedly, Su-13437 stabilizes lysosomes. Our results suggest that matrix extraction and increased soluble enzyme activities result from transmembrane passage of peroxisomal proteins.

The changes in concentration of peroxisomal oxidases and soluble catalase after Su-13437 allow the calculation of their half-lives. These are the same as those found for total catalase, in normal and treated rats, after allyl isopropyl acetamide: about 1.3 days, a result compatible with peroxisome degradation by autophagy. A sequential increase in liver RNA concentration, [ $^{14}\text{C}$ ]leucine incorporation into DOC-soluble proteins and into immunoprecipitable catalase, and an increase in liver size and peroxisomal volume per gram liver, characterize the trophic effect of the drug used. In males, Su-13437 is more active than CPIB, another peroxisome proliferation-inducing drug; in females, only Su-13437 is active.

Peroxisomes are cell organelles, widely distributed in eucaryotic cells, whose function is partially known only in protists (48) and plants (6, 29, 59). Their role in animal tissues is not known, in spite of the various physical, morphological, and biochemical analyses to which they have been subjected (2, 16, 31, 42, 43). Most of the work has concentrated on rat liver peroxisomes, but their set

of known enzymes has not yet been assigned a precise or unique place in metabolism. Moreover, their reduced response to multiple physiological and pathological conditions (31, 57, 58) gives no indication of to which cell function they might be related. In fact, peroxisomes have been considered as fossil organelles in animal tissues (15). If that were so, they would constitute expensive fossils since they account for 2.5% of the liver protein and have a high turnover rate that has been confirmed in the present work (43, 52). The hypothesis thus remains a challenge to cell biologists.

The induction of proliferation of peroxisomes by some drugs constitutes an exception to their apparent inertness in the cell and is a potential tool for exploring their function. Particularly active are a group of hypolipidemic drugs that induce liver growth in rats; and some of them inhibit auxin-promoted growth in plants (1). *p*-Chlorophenoxy isobutyrate (CPIB)<sup>1</sup> has been the most widely used (25, 58). Several years ago we selected Su-13437, another drug from the group, to study peroxisome proliferation, with the aim of establishing the temporal course of the early changes and facilitating in this way the correlation between increased peroxisomal mass and its eventual physiological activities.

Su-13437 proved to be more active than CPIB, not only in this respect but also as an antiauxin (39), as well as with respect to its known effect on plasma lipid levels (9, 23, 24, 34, 35). A report confirming the proliferation of peroxisomes and the induction of higher levels of total catalase with Su-13437 has been published recently (54). In the present work we show that proliferated peroxisomes are different from normal peroxisomes: their known enzymes are strikingly reduced or suppressed, while the peroxisomal volume per gram liver increases several-fold. For the first time, a specific determination of the turnover of peroxisomal oxidases has been made, together with that of catalase and soluble catalase after Su-13437, yielding values compatible with simultaneous degradation. We also present evidence that

the content of proliferated peroxisomes is extracted, presumably through the membrane, during tissue fractionation, a phenomenon that also affects normal peroxisomes and that should be taken into account in the evaluation of the isolation procedures and in the determination of the subcellular localization of peroxisomal enzymes. Preliminary communications of some of these results have been made (39-41).

## MATERIALS AND METHODS

### *Drug Administration and Preparative Procedures*

Male Sprague-Dawley rats, weighing 200-250 g, were used. In the series in which the influence of sex was studied females of about the same weight were used. Su-13437 was administered in a dose of 1 g, and CPIB in a dose of 3 g per kg rat chow, respectively. The animals were kept in a room with controlled temperature and constant 12-h daily cycles of artificial illumination. The administration of the drug was started at 7-9 p.m. Rats were always killed between 9 and 10 a.m. by decapitation, without previous fasting. The livers were homogenized after mincing, in 3 vol of 0.25 M sucrose at 0°C with two strokes of a Potter-Elvehjem homogenizer. Ethanol 0.1% was routinely added to the sucrose solutions to protect catalase activity (42). The homogenate was further diluted to 1:10 wt/vol, filtered through a double layer of surgical gauze, and aliquots of 10 ml were submitted to an integrated force of 380,000 g-min (17), in the outer row of an SM-24 Sorvall rotor by spinning for 10 min at 20,000 rpm. Under these conditions, the maximal hydrostatic pressure to which the pellet was subjected was 108 kg/cm<sup>2</sup>. The supernate from this single-step, simplified fractionation procedure will be referred to as the supernatant fraction, and the pellet as the particle-bound fraction. This procedure gives a complete sedimentation of peroxisomes and a supernatant fraction with some microsomes (17). Regular mitochondria plus light mitochondria (ML) particulate fractions and complete fractionations were made as described by de Duve et al. (18); the speed selected to sediment the ML pellet resulted in a maximal hydrostatic pressure of 125 kg/cm<sup>2</sup> at the bottom of the centrifuge tube.

### *Biochemical Determinations*

Protein was measured by the method of Lowry et al. (45). DNA was determined with diphenylamine according to Burton (13). RNA was measured with the procedure of Fleck and Munro (21). Cytochrome oxidase and urate oxidase were assayed as previously described (42). Acid phosphatase was measured according to de Duve et al. (18). For catalase, the assay used by Baudhuin et al. (3) was employed. L-alpha-hydroxy acid oxidase and D-amino acid oxidase were determined with

<sup>1</sup> *Abbreviations used in this paper:* AIA, allyl isopropyl acetamide; CPIB, *p*-chlorophenoxy isobutyrate; DAB, 3,3'-diaminobenzidine; DOC, sodium deoxycholate; ML, mitochondria plus light mitochondria subcellular fraction; N, nuclear subcellular fraction; P, microsomal subcellular fraction; S, soluble subcellular fraction (all fractions prepared as described in reference 18); Su-13437, 2-methyl-2-(*p*-(1,2,3,4-tetrahydro-1-naphthyl)-phenoxy)-propionic acid; TCA trichloroacetic acid.

L-lactate and D-alanine by a modification of the procedure described by Neims (49), forming and measuring the pyruvate dinitrophenylhydrazine at 15°C. Units are expressed as micromoles of pyruvate formed in 1 min per gram liver.

### Peroxisome Fragility

Fragility was evaluated by morphological analysis, as described below, and from the change in the soluble fraction of catalase for peroxisomes, and acid phosphatase for lysosomes. Lysosomes were included as a control. 0.25 M sucrose, with 0.1% ethanol, was used as the homogenization medium unless stated otherwise. Homogenates were prepared and kept at 0°C, but the activity and distribution of both marker enzymes were not modified when proceeding at 20°C or 37°C. Homogenizations were made with the same homogenizer, at 1,200 rpm. for all fragility experiments; however, the use of 10-, 30-, or 55-ml homogenizers had no effect on the distribution of catalase or of acid phosphatase. The effect of prolonged homogenization was studied increasing the number of strokes from 2 to 19. The effect of increased viscosity was explored with 1.8 M sucrose as the homogenization medium.

### Morphological Observations

Fixation for electron microscopy was made with 1.33% OsO<sub>4</sub> buffered with 0.66 M *s*-collidine, pH 7.6, for 2 h (7). This fixative was adopted because of the high density it imparts to the peroxisomal matrix and nucleoid. Block staining with 2% aqueous uranyl acetate was done routinely with tissue blocks and pellet samples. The sections, stained with lead citrate (62), were observed in a Siemens Elmiskop 1A electron microscope. Pellets were processed as follows: after gentle manual mixing in the sedimentation tube with a glass rod, a sample was suctioned with a glass pipette and droplets of about 0.5 mm diameter were slowly released into cold fixative; after 30 min, they could be handled as tissue blocks. Larger droplets should not be used since the penetration of the fixative becomes limiting. For histochemical analysis of peroxidative activity, fixation was made in Karnovsky's fixative (33), and the DAB procedure of Graham and Karnovsky, as modified by Novikoff and Goldfischer (50), was applied. Morphometric determinations of the maximal diameter of peroxisomal sections were made directly on the prints, one measurement per particle, in such a way that all recorded diameters were parallel to one of the edges.

### Protein Turnover Analysis

We assume that the changes observed in the activity of peroxisomal enzymes were due to modifications of their rate constants of synthesis or degradation. Therefore, the changes have been treated in various ways, in agreement with the general theory of protein turnover in cells (55).

The following general equation (8) was used for the

analysis of changes in enzyme levels:

$$E_t = \frac{k_s}{k_d} - \left( \frac{k_s}{k_d} - E_0 \right) e^{-k_d t} \quad (1)$$

$E_0$  and  $E_t$  are, respectively, the initial and the final enzyme concentrations;  $k_s$  the zero order rate constant of synthesis;  $k_d$  the first order rate constant of degradation, and  $t$ , the time at which  $E_t$  is measured. The equation reduces to a simple exponential if  $k_s/k_d$  becomes very small or zero. For a given experimental system in steady state,  $k_s/k_d$  can be measured since it is equal to the enzyme concentration. The rate constant of degradation  $k_d$  can thus easily be estimated following the evolution of enzyme concentration, on a semilogarithmic plot, while the system changes to a new steady state level (22). In practice, we have assumed that steady state was reached after 6.5 days of drug administration. For catalase after AIA (53) and the change in D-amino acid oxidase activity, a steady state level of 0 was assumed.

### Incorporation of [<sup>14</sup>C]Leucine in vitro into Catalase and Liver Proteins

Leucine incorporation in liver slices was used to evaluate the effects of Su-13437 on the rate of synthesis of catalase and DOC-soluble liver proteins. One determination, with a single slice weighing about 80 mg, was made for each rat; to minimize variations, the dimensions of the slices were constant. Incubation was carried out at 37°C for 1 h in 1 ml Krebs-Ringer phosphate medium (61) containing 1.25 μCi of DL-[<sup>14</sup>C]leucine (25.6 mCi/mmol), in an atmosphere of 95% oxygen and 5% carbon dioxide, in a shaking bath at 60 cycles per minute. After washing at 4°C with leucine-free medium, the slice was homogenized with 2 ml of 0.6% DOC in 0.05 M, pH 8.0, Tris buffer. The supernate, after centrifugation for 25 min at 45,000 rpm, contained all the catalase and the DOC-soluble liver proteins.

Immunoprecipitation of catalase from the DOC extract was accomplished with rabbit anti-rat liver catalase antiserum. Pure rat liver catalase for immunization was prepared as previously described (43). The preparation of antiserum and the immunoprecipitation were carried out essentially as described by Higashi and Peters (26). The DOC extract, 0.4 ml, was mixed with 0.2 ml of crude antiserum and the immunoprecipitate resulting after 1 h at 37°C and 36 h at 4°C was washed three times with 0.15 M NaCl and dissolved in 0.5 N NaOH. A 0.1-ml sample was used for protein determination (45), and the rest for radioactivity measurement after reprecipitation with TCA in presence of 1 mg of bovine serum albumin. Protein precipitates for radioactivity counting were collected on glass fiber paper, Whatman GF/C, and after dehydration the radioactivity was determined by liquid scintillation in 10 ml of 0.4% BBOT (Packard Instrument Co., Downers Grove, Ill.) in toluene.

The sensitivity of the overall procedure was checked with two rats 25 h after subjecting them to a 70% partial hepatectomy. A 66% increase in specific activity of the DOC-soluble liver protein was found, but no significant incorporation into immunoprecipitable catalase was detected. In fact, hepatectomy induces an early and transient drop in catalase activity (36) that is compatible with a block of its synthesis during the period studied. There are some uncertainties involved in immunoprecipitation of catalase from rat liver (52), since the catalase antigens present are heterogeneous (37, 38). Anyhow, the dissociation observed in regenerating liver constitutes an argument for excluding contamination as the explanation for the label in the immunoprecipitate.

### Statistical Calculations

Single group results are expressed as averages  $\pm$  standard deviation. Two group comparisons have been made applying Student's *t* test. A chi square test was also applied to the frequency of peroxisomal matrix extraction. The semilogarithmic plots for turnover analysis were derived from first class linear regression analysis, with 95% confidence intervals calculated from the variance of the slope.

### Chemicals

Substrates and reagents for chemical and histochemical enzyme determinations were obtained from Sigma Chemical Co., St. Louis, Mo., and chemicals of general use from E. Merck A. G. Isotopes were obtained from New England Nuclear, Boston, Mass. Electron microscopy reagents were purchased from E. F. Fullam Inc., Schenectady, N. Y. Su-13437 was supplied by Farbwerke Hoechst A.G. and CPIB by Ayerst Laboratories, New York.

## RESULTS

### Body and Liver Growth

At 0.1% in the diet, Su-13437 markedly affects body growth (Fig. 1). In contrast, the fraction of body weight corresponding to the liver increases from  $4.4 \pm 0.1$  to  $6.3 \pm 0.7$ . This change in relative mass is due to an absolute increase in the rate of liver growth, maximal between 0.5 and 3.5 days (Fig. 2), and to a decreased rate of body growth.

### Liver Composition

Different biochemical components of the liver were measured at 0, 0.5, 1.5, 2.5, 3.5, and 6.5 days after treatment. DNA remains constant with experimental values not significantly different from the control value,  $1.29 \pm 0.18$  mg/g liver. Protein concentration was also maintained within normal values:  $159 \pm 14$ ,  $86 \pm 3$ , and  $71 \pm 5$  for total,

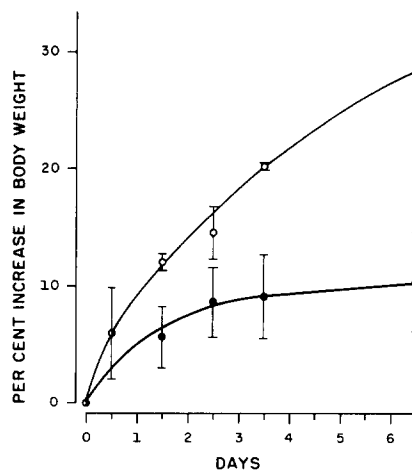


FIGURE 1 Body growth in control (open circles) and Su-13437-treated rats (filled circles). Two animals per point in the control and four in the treated groups. In all figures, vertical bars over and below the average points represent one standard deviation.

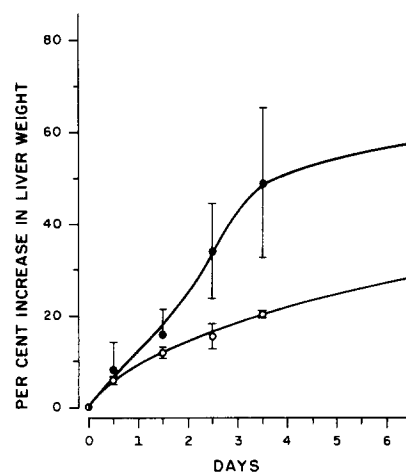


FIGURE 2 Liver growth in control (open circles) and Su-13437-treated rats (filled circles). The curves were calculated from the body growth data and the average body weight fraction corresponding to the liver at various intervals. Treatment increases the fraction of body weight corresponding to the liver from  $4.4 \pm 0.1$  to  $6.3 \pm 0.7$ .

particle-bound, and supernatant activities in milligrams per gram liver. The concentration of RNA changes rapidly, reaching a peak value, 20% over the control, after 0.5 day (Fig. 3). Marker enzymes for some cell organelles were followed: acid phosphatase values for total, particle-bound, and supernatant activities were not different from the control

values  $3.73 \pm 0.46$ ,  $2.41 \pm 0.90$ , and  $0.52 \pm 0.13$  U/g liver, respectively; however, as shown later, there was some effect on the distribution of the enzyme. Cytochrome oxidase rose slowly from the normal value,  $31.9 \pm 5.7$  U/g liver, at a statistically significant average rate of 1.1 U per day, during the 6.5 days of observation.

The most striking biochemical effects after Su-13437 administration were detected on peroxisomal enzymes. The total activity for each of the oxidases gradually decreases on a gram liver weight basis, while that of catalase increases. The increase in catalase activity results from the algebraic sum of a severalfold increase in the supernatant fraction of the enzyme, plus a marked reduction in the particle-bound fraction (Fig. 4). Urate oxidase decreases by approximately 40% (Fig. 5). L-Alpha-hydroxy acid oxidase decreases by approximately 70%, and D-amino acid oxidase practically disappears (Fig. 6 and Fig. 7); for both enzymes the change affects the supernate and particle-bound activities.

#### Comparative Effects of Su-13437 and CPIB and Influence of Sex

A comparative study of the effect of Su-13437 and of the chemically and pharmacologically related drug CPIB was carried out on rats of both sexes. Su-13437 was administered at the regular dose of 1 g per kg chow and CPIB at 3 g per kg, a

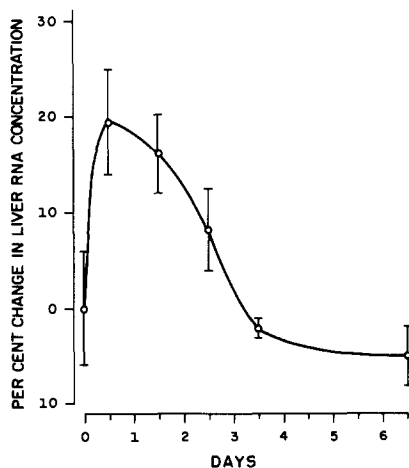


FIGURE 3 RNA concentration in liver during Su-13437 administration. Control rats have  $10.4 \pm 0.6$  mg RNA per gram liver. The points under treatment correspond to 4 rats, 10 rats for the control. Levels at 0.5 and 1.5 days differ significantly from control values;  $P < 0.001$ .

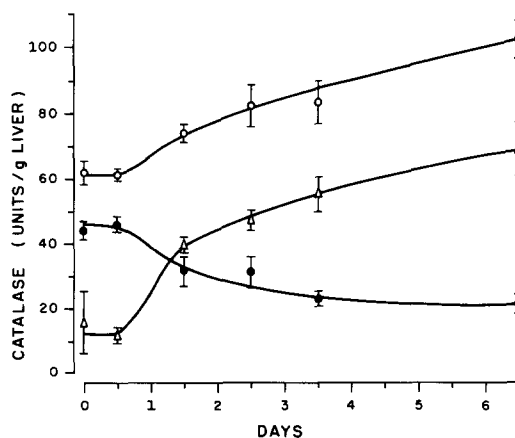


FIGURE 4 Catalase activity in liver during Su-13437 administration. Total (open circles), particle-bound (filled circles) and soluble activities (triangles). Each point is the average of four rats.

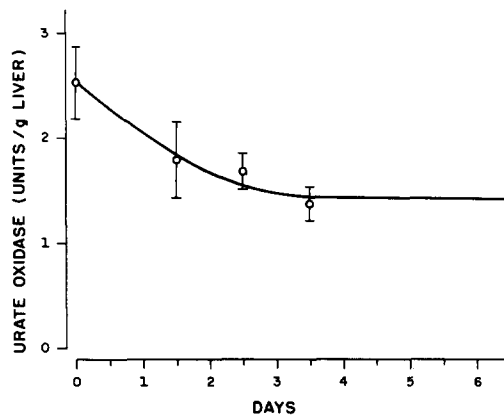


FIGURE 5 Urate oxidase activity in liver during Su-13437 administration. Each point is the average of four rats.

dose commonly used in experimental studies with this drug. The results, shown in Table I, demonstrate that both drugs, administered during 6.5 days, have similar qualitative effects on the activity and distribution of peroxisomal enzymes. The changes induced are larger in male rats. In this particular experimental series, only Su-13437 induced an increase in catalase activity of male liver, although both drugs increased the supernatant fraction. This reduced response is not due to errors in the administration of the drug, since the oxidases show the usual decrease in concentration. In fact, in our laboratory, the response of this enzyme to Su-13437 has an apparently seasonal fluctua-

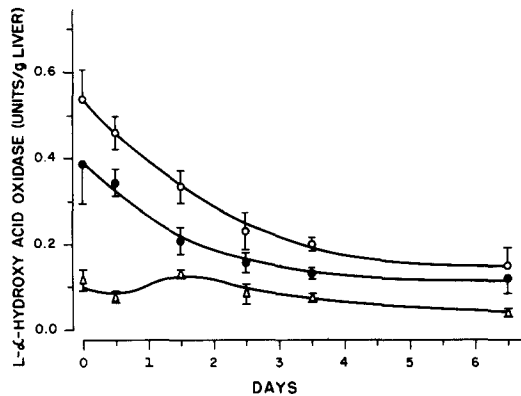


FIGURE 6 L-Alpha-hydroxy acid oxidase activity in liver during Su-13437 administration. Total (open circles), particle-bound (filled circles), and soluble activities (triangles). 10 rats for the control level, and 4 for each point under treatment.

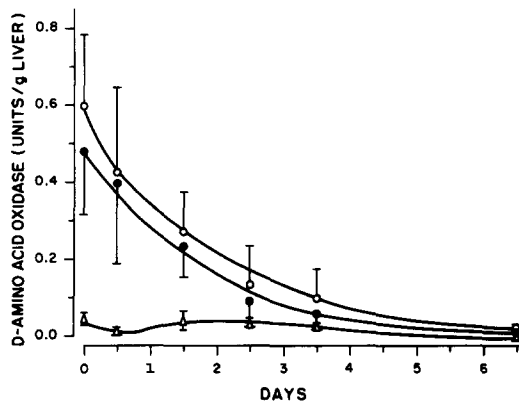


FIGURE 7 D-Amino acid oxidase activity in liver during Su-13437 administration. Total (open circles), particle-bound (filled circles), and soluble activities (triangles). 10 rats for the control level, and 4 for each point under treatment.

tion. Higher induced levels are found in winter. The results shown in Table I were obtained in summer while those from Fig. 4, where a marked effect on catalase is illustrated, were obtained in winter. In another observation made in winter, the effects of both drugs were compared in groups of six male rats. The following values were found: control,  $52.1 \pm 3.3$  U; Su-13437-treated,  $96.3 \pm 4.8$  U; CPIB-treated,  $66.5 \pm 7.0$  U. The fluctuation could be due to changes in the diet composition, but we have no evidence to prove it. At any rate, to account for it, control values were always obtained simultaneously with the experimental groups.

The activity of D-amino acid oxidase is almost completely suppressed in both males and females by Su-13437, while CPIB exerts only a moderate effect. The activities of urate oxidase and L-alpha-hydroxy acid oxidase are also depressed by Su-13437 in males and females, while CPIB, which in males is less active, exerts no influence in females.

Whenever the drugs have some effect on the concentration of peroxisomal enzymes there is a shift in their distribution, a larger fraction of the catalase and the soluble oxidases appearing in the supernate. Urate oxidase always remains insoluble or particle bound.

We may conclude that both drugs affect the level and distribution of peroxisomal enzymes. Su-13437 is more active than CPIB; both act on male rats, while only Su-13437 shows a clear effect on the peroxisomal enzymes of the females.

### Liver Structure

A rough estimation of the frequency, size, and distribution of peroxisomes can be obtained from a

TABLE I  
Effect of Su-13437 and CPIB on the Activity and Distribution of Liver Peroxisomal Enzymes. Male and Female Rats Treated for 6.5 Days

	Catalase		DAAO		LαHAO		Urate oxidase
	U/g	% in S	U/g	% in S	U/g	% in S	U/g
<b>Males</b>							
Control (4)*	61.1 ± 4.5†	29.1 ± 3.2	0.535 ± 0.208	12.8 ± 2.5	0.503 ± 0.093	20.8 ± 3.1	3.22 ± 0.45
Su-13437 (4)	74.5 ± 4.5	63.3 ± 7.0	0.032 ± 0.021	30.9 ± 24.0	0.164 ± 0.023	42.2 ± 5.0	1.48 ± 0.19
CPIB (4)	59.0 ± 5.1	50.2 ± 3.3	0.148 ± 0.026	32.7 ± 4.2	0.248 ± 0.021	37.0 ± 2.6	1.92 ± 0.15
<b>Females</b>							
Control (4)	30.1 ± 2.0	25.8 ± 8.0	0.441 ± 0.124	8.8 ± 4.4	0.255 ± 0.044	17.4 ± 4.7	3.99 ± 0.17
Su-13437 (4)	53.1 ± 2.6	46.7 ± 4.9	0.057 ± 0.010	20.2 ± 6.6	0.173 ± 0.017	25.1 ± 3.2	2.90 ± 0.15
CPIB (4)	40.8 ± 6.0	16.4 ± 3.5	0.302 ± 0.130	6.1 ± 1.7	0.284 ± 0.013	12.8 ± 2.5	3.61 ± 0.51

\* Number of individual determinations.

† Average value ± SD.

DAAO = D-amino acid oxidase.

LαHAO = L-alpha-hydroxy acid oxidase.

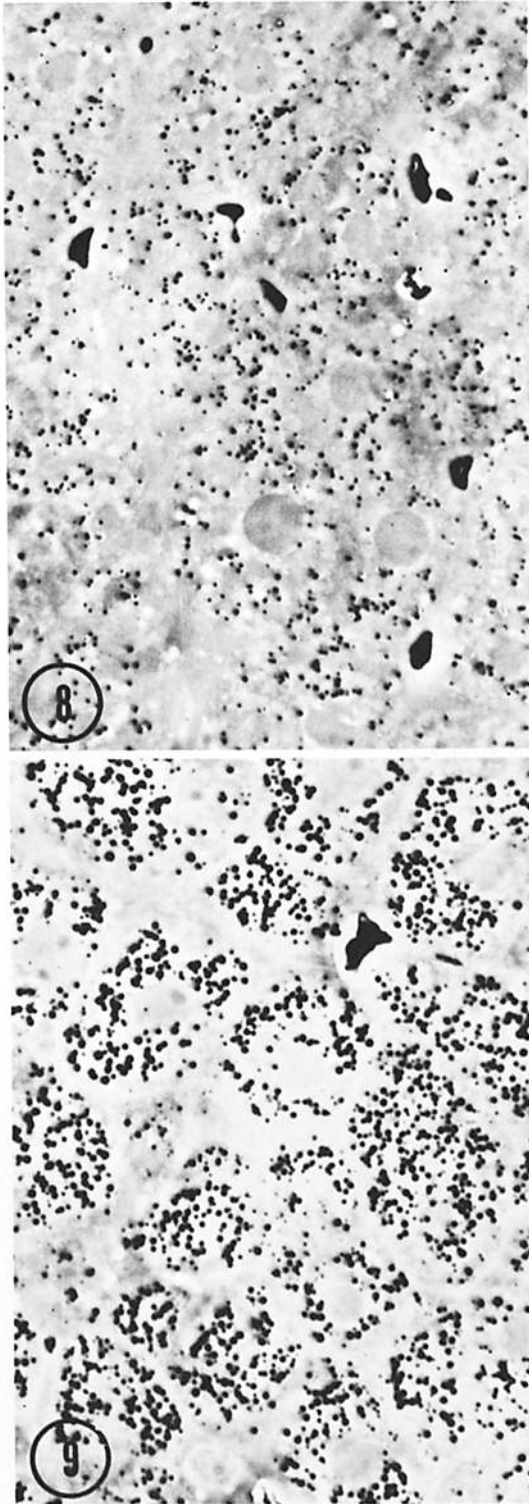


FIGURE 8 and 9 Thick sections through Epon-embedded liver tissue after incubation with 3,3'-diaminobenzi-

thick section of Epon-embedded tissue after histochemical detection of peroxidative activity with DAB. As shown in Fig. 8, in normal liver cells, peroxisomes appear as isolated particles or small linear clusters distributed at random in the cytoplasm. In hepatocytes from treated rats (Fig. 9), they are more numerous, bigger, and distributed at random in the entire cytoplasmic area; in this case, clusters are difficult to detect because of the high frequency of peroxisomes.

The relative frequency and structural characteristics of normal peroxisomes under the electron microscope are illustrated in Fig. 10. The organelles show a finely granular matrix, with the same electron density for all particles, that often contains a heavily stained nucleoid. The average diameter of sections through normal peroxisomes was found to be  $0.58 \pm 0.15 \mu\text{m}$  (Table II). Normal peroxisomes give a positive DAB peroxidatic reaction, with approximately the same concentration or density of the reaction product in all particles (Fig. 11). Starting at 1.5 days after treatment, Su-13437 induces changes in the liver structure: as illustrated in Fig. 12, continuities between the peroxisomal membrane and membrane fragments that look like smooth endoplasmic reticulum profiles are more frequent. The nucleoid, which will later transiently disappear from almost all proliferated peroxisomes, frequently looks partially disaggregated, and is occasionally seen free in the cytoplasm. Also, after 1.5 days, and not at other time intervals, practically all lipid droplets are almost completely surrounded by smooth endoplasmic reticulum profiles.

After 3.5 days of treatment, the morphologic characteristics of proliferated peroxisomes are clearly different from those of normal particles. The peroxisomes look the same after 6.5 days, except that the nucleoid, practically absent after 3.5 days, is again occasionally seen (Fig. 13). Peroxisomes are bigger, some having a diameter of  $1 \mu\text{m}$  or more, and present a variable electron density of the matrix in different particles. The average diameter of sections through proliferated particles is  $0.73 \pm 0.25 \mu\text{m}$ . Those with very low electron density were identified as peroxisomes

dine (DAB), to detect peroxidatic activity. Peroxisomes and red blood cells show a positive reaction. Fig. 8 corresponds to a normal rat and Fig. 9 to a rat treated with Su-13437 for 6.5 days. The increase in number and size of peroxisomes is clearly detectable.  $\times 1,650$ .

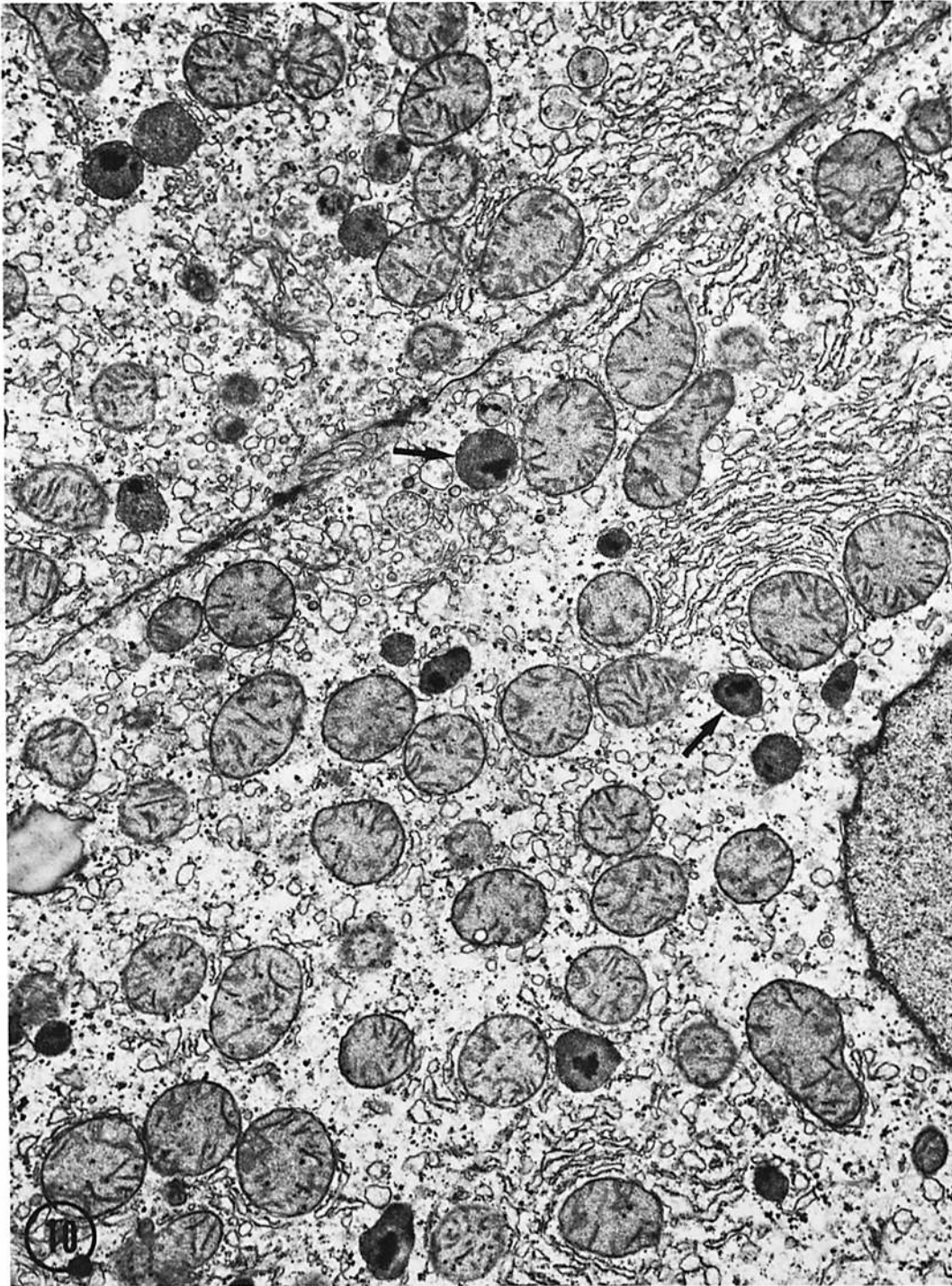


FIGURE 10 Normal rat liver. The section illustrates the morphological characteristics of peroxisomes in tissue fixed with *s*-collidine-buffered osmium tetroxide. Peroxisomes (arrows) show a heavily stained nucleoid and a finely granular matrix. They are smaller and less numerous than mitochondria.  $\times 12,000$ .



TABLE II  
Diameter of Peroxisomal Sections in Liver and in Tissue Fractions\*

Sample	Controls	Su-13437	P
	$\mu\text{m}$	$\mu\text{m}$	
Liver tissue	$0.58 \pm 0.15\ddagger$	$0.73 \pm 0.25$	$<0.005$
Pellet from single step fractionation	$0.59 \pm 0.15$	$0.69 \pm 0.21$	$<0.010$
Pellet from ML fraction	$0.56 \pm 0.15$	$0.69 \pm 0.18$	$<0.001$

\* An average of 68 peroxisomal sections, randomly selected, was used for each group.

† Results are expressed as average diameter, in  $\mu\text{m} \pm \text{SD}$ . P for the differences was calculated applying Student's *t* test.

after a positive DAB reaction had been found, as shown in Fig. 14, at all time intervals. In contrast to normal particles, proliferated peroxisomes often show a variable concentration or density of DAB peroxidative product; the larger sections, which usually correspond to the low electron density particles, show less reaction product than the small forms. There are also areas where all proliferated peroxisomes have a very homogeneous histochemical reaction, as shown in Fig. 15. This micrograph also shows proliferation of the smooth endoplasmic reticulum, a phenomenon also apparent in Fig. 13 where the profiles appear fragmented, presumably because of the different fixation employed. Since our attention was focused on the morphological changes that are detected while normal peroxisomes are being replaced by proliferated ones, the results of chronic administration of Su-13437 were checked at only one time interval, 45 days. The main findings after chronic administration are shown in Fig. 16: the nucleoid is again present, and peroxisomes have either a normal matrix or a flocculent, low electron density content. Mitochondria, after chronic treatment, show abnormal aggregation of cristae.

Peroxisome-containing autophagosomes were seen occasionally in both control and treated rats (Figs. 17, 18). Their frequency was low and no correlation could be established with the administration of Su-13437.

#### *Physical Properties of Proliferated Peroxisomes. Biochemical and Morphological Observations*

The subcellular distribution of peroxisomal enzymes during Su-13437 administration suggests

that the organelle is no longer able to retain its contents. Fig. 19 shows the average change in distribution of peroxisomal enzymes, excepting urate oxidase which is not soluble. The increase in the supernatant fraction of catalase is remarkable for its magnitude and also for the small scattering of individual values, as reflected in the standard deviations. L-alpha-hydroxy acid oxidase and D-amino acid oxidase also increase in the supernate, but less than catalase. The increase for D-amino acid oxidase is not statistically significant; a large scattering of values resulted from calculation of the ratio of residual activities. The shift in enzyme distribution does not affect the bulk of cell organelles since the protein distribution is not changed; in fact, for acid phosphatase, precisely the opposite effect is found (Fig. 20).

In order to explore an eventual increase in the fragility of proliferated peroxisomes, leading to a larger fraction of broken or disrupted particles after homogenization, the procedure was carried out under more severe conditions: prolonged exposure to shearing forces by homogenization with 19 instead of 2 strokes; and homogenization in a viscous medium to increase shearing forces: 1.8 M sucrose, equivalent to a 20-fold increase in viscosity. Adequate controls were used for the latter condition, since the final sucrose concentration after homogenization and dilution was 0.43 M. Rats treated for 3.5 days were used, since that time appears to be the moment of maximal fragility and at that time the oxidases have not yet reached their minimum level.

The results shown in Table III indicate that catalase was slightly released by prolonged homogenization in control but not in treated rats. However, in 1.8 M sucrose, almost two-thirds of the catalase is present in the supernate from control rats; in treated rats, there was a further increase, but not a statistically significant one, of the already large soluble fraction. Acid phosphatase distribution was not affected by prolonged homogenization; but, in the viscous medium, there was a minor release, slightly higher for the controls. The supernatant fraction of acid phosphatase, in control and severe homogenization conditions, is always slightly lower for treated rats. This correlates with the temporal course of acid phosphatase distribution that shows a decrease in the supernatant fraction (Fig. 20). Therefore, a minor but significant apparent stabilization of lysosomes follows drug administration, precisely the opposite

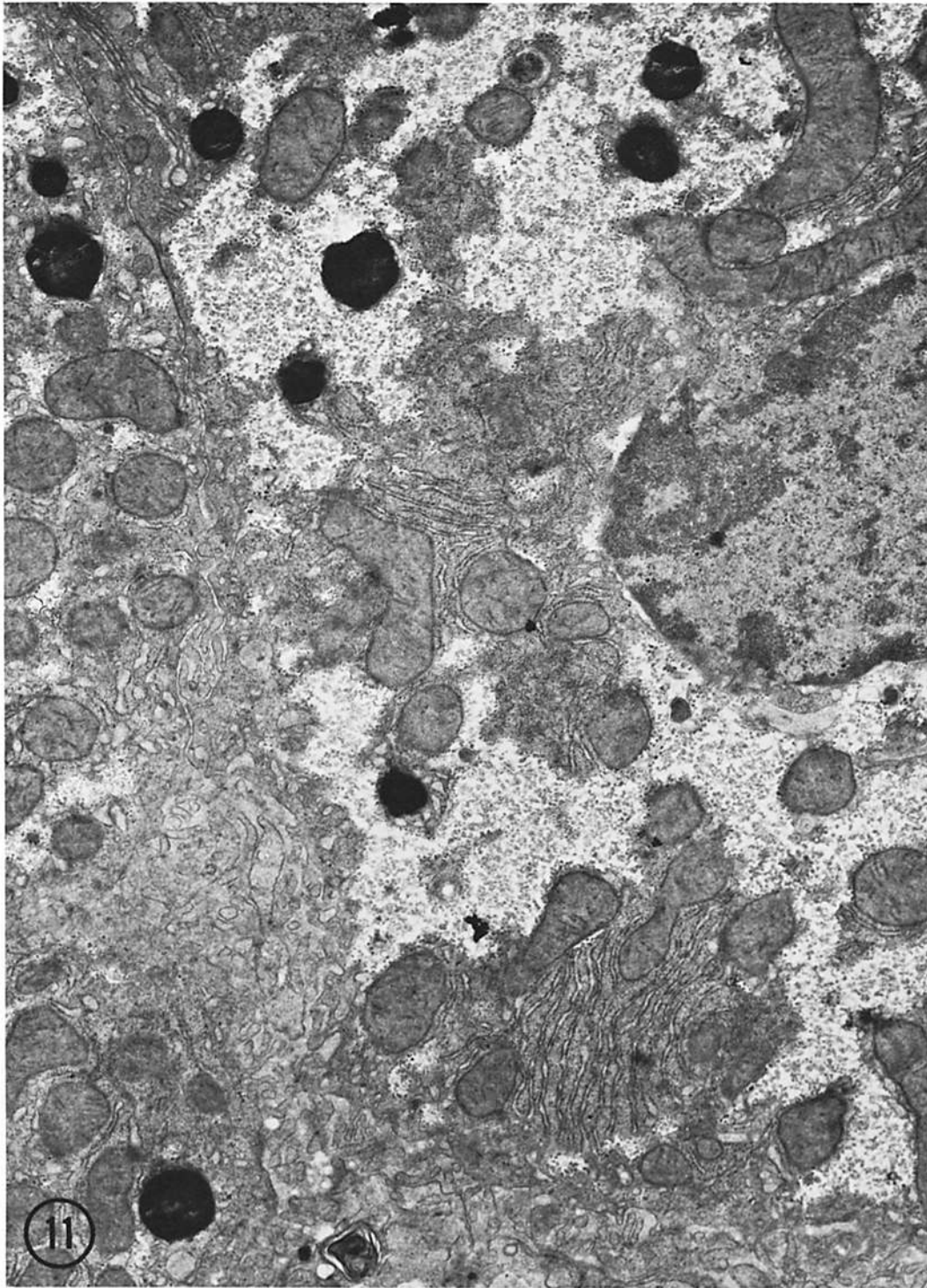


FIGURE 11 DAB peroxidation in control liver. The peroxisomes are selectively stained by the reaction product.  $\times 15,000$ .

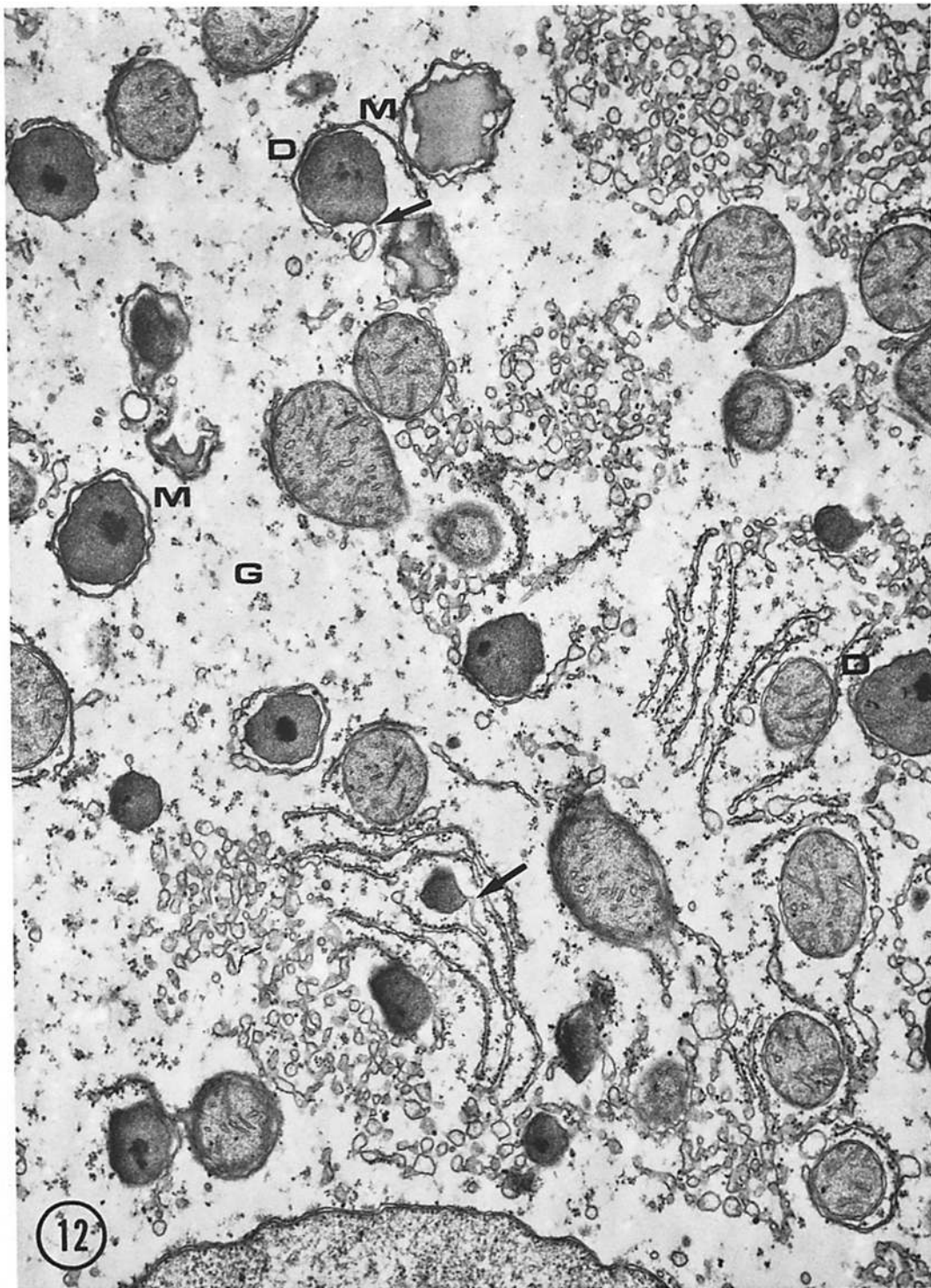


FIGURE 12 Hepatocyte structure after 1.5 days of Su-13437 administration. Continuities between peroxisomes and smooth membrane profiles are detected (arrows). Partial disaggregation of the nucleoid is seen in two particles (*D*), illustrating the temporal disappearance of the structure that follows treatment. Smooth endoplasmic reticulum profiles (*M*) were frequently seen around peroxisomes and lipid droplets at this stage. The background (*G*) corresponds to a glycogen area which is not stained with the fixative and stains employed.  $\times 18,000$ .

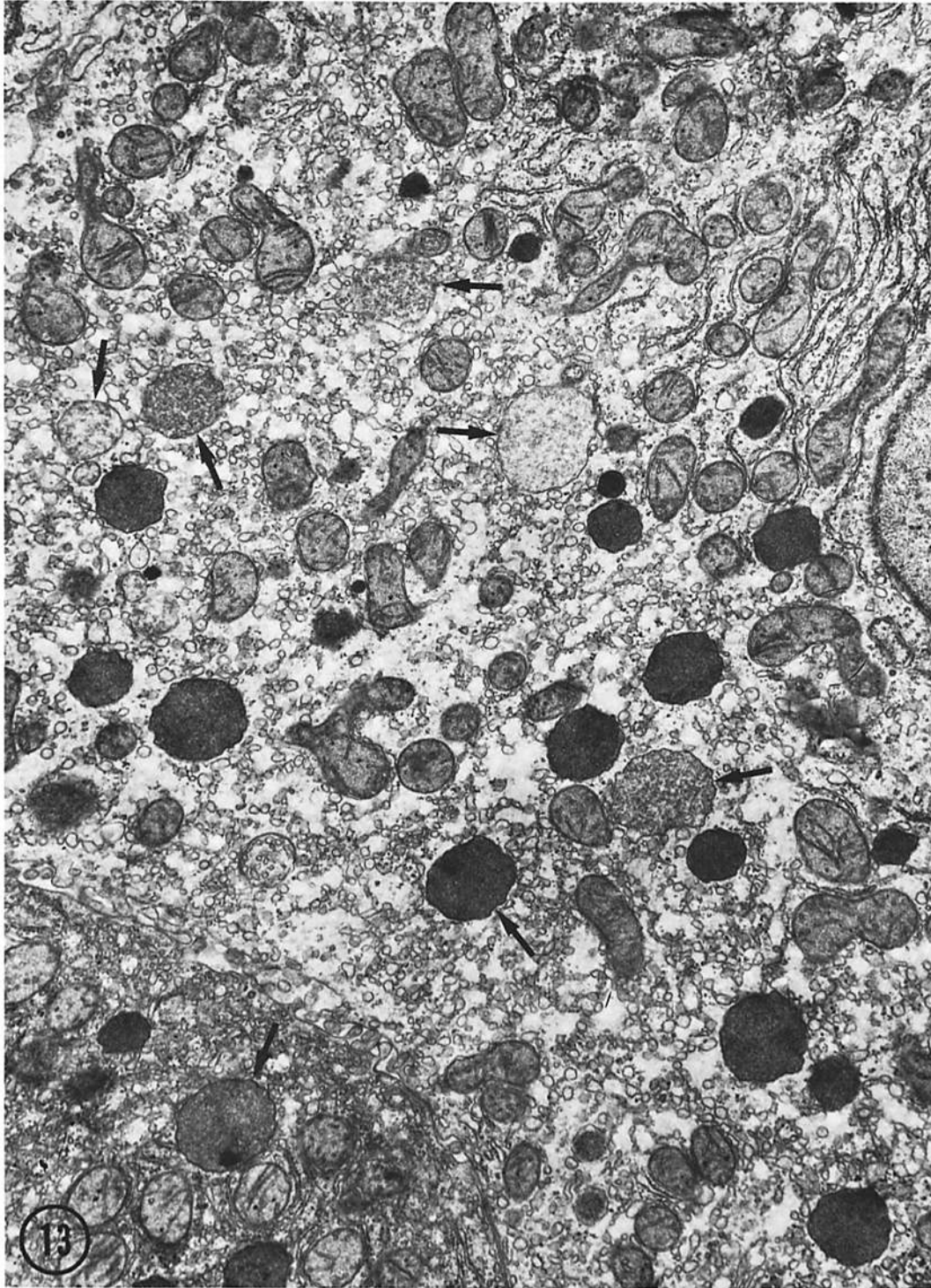


FIGURE 13 Liver structure after 6.5 days of Su-13437. Peroxisomes are pleomorphic, more numerous, and larger, even larger than mitochondria. The electron density of the matrix is not the same in different particles (arrows). Nucleoids are practically absent. There is a moderate proliferation of the smooth endoplasmic reticulum, which also appears fragmented.  $\times 12,000$ .

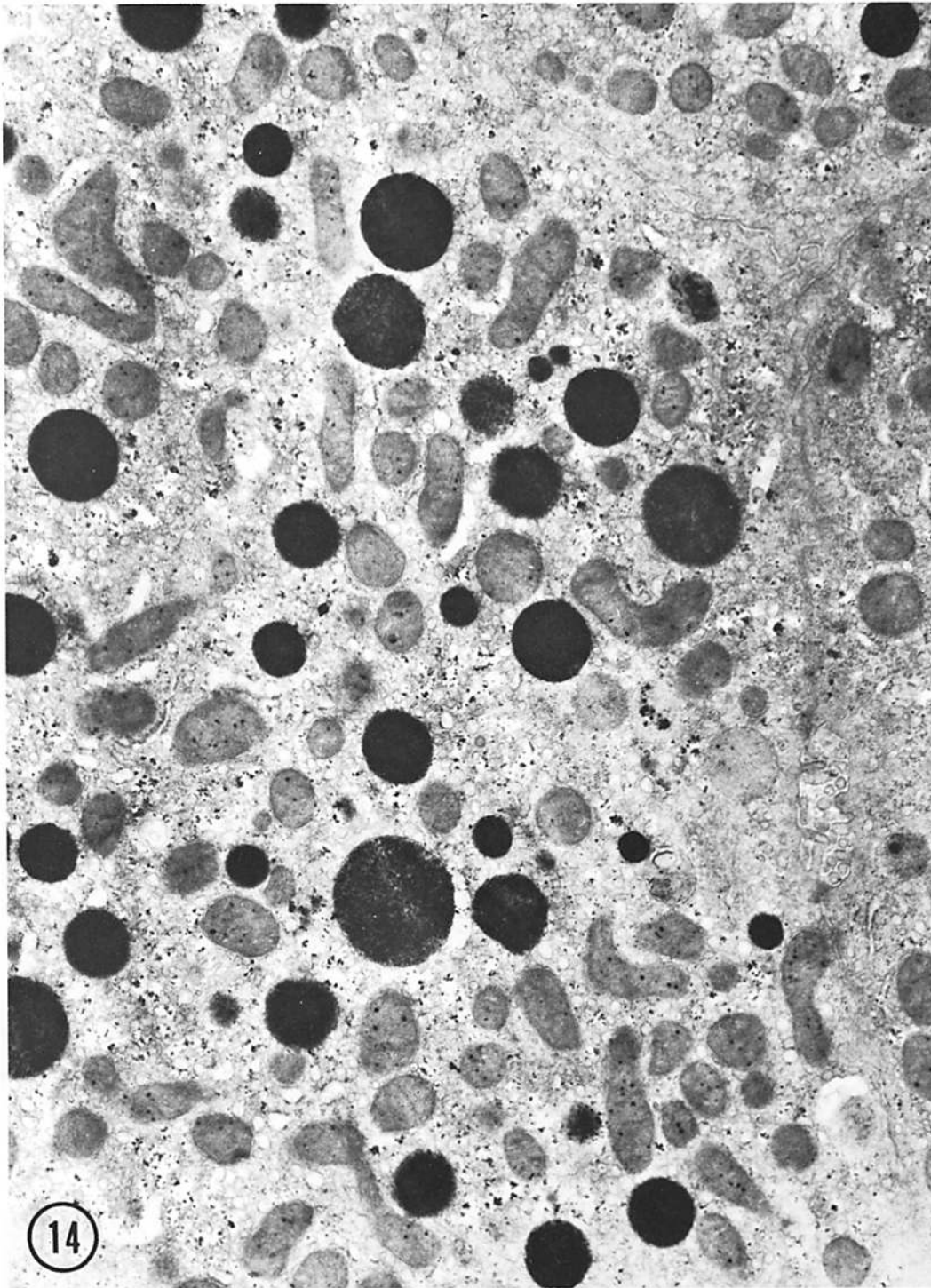


FIGURE 14 DAB peroxidation in rat liver after 6.5 days of Su-13437. In this section, the numerous proliferated peroxisomes show circular profiles that contrast with those illustrated in Fig 15. The size distribution of peroxisomes is much wider than that observed in control liver; several particles have a diameter larger than  $1 \mu\text{m}$ , but there are also many small particles. The intensity of the DAB peroxidation product is higher in the smaller particles, a peculiar property of proliferated peroxisomes.  $\times 13,500$ .

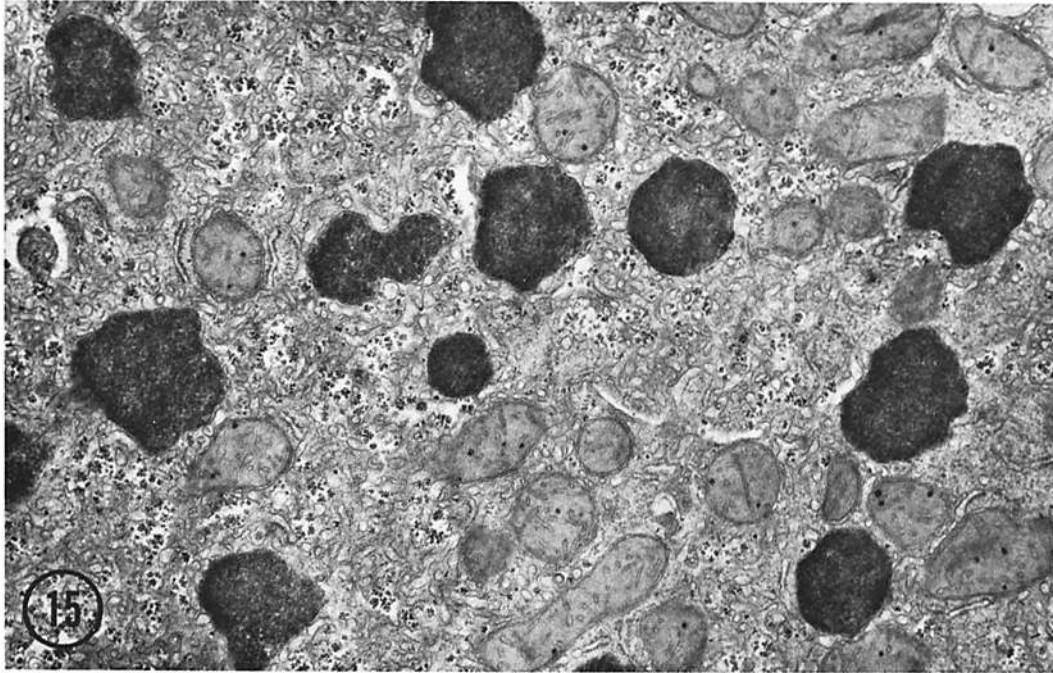


FIGURE 15 DAB peroxidation in rat liver after 6.5 days of Su-13437. In this section, proliferated peroxisomes show a uniform deposit of reaction product and an irregular profile that is often present after treatment. The smooth endoplasmic reticulum appears proliferated, but not fragmented into vesicles as in Fig. 13, presumably because of the aldehyde fixation used for histochemistry.  $\times 20,000$ .

effect postulated for peroxisomes. The distribution of protein was not modified by drug administration under any of the tests, but the amount sedimenting in 0.43 M sucrose is less than in 0.25 M, a result to be expected since, in spite of the increase in viscosity, density, and osmolarity of the medium, the same integrated force was applied for sedimentation. We may conclude that, under conditions leading to a partial release of particle-bound catalase, the peroxisomes present in the particulate fraction of treated rats did not show more fragility than those from control rats.

The absence of a detectable increase in peroxisomal fragility does not rule it out. The particles resisting the fractionation could be the stronger ones, while labile particles would be disrupted already under normal homogenization and fractionation conditions. Then the effect of Su-13437 would be to increase the fraction of labile particles. Many proliferated peroxisomes are in fact bigger and might contain a major portion of the enzymes; further, they should be mechanically more labile than small forms. To determine if large peroxisomes are selectively broken during fractionation, the diameter of sections through the organelle in

liver of normal and treated rats was compared with that of sections through peroxisomes present in particulate fractions, after the single-step fractionation and in the ML fraction of the multiple step procedure. As shown in Table II, the diameter of peroxisomal sections was the same, in control and treated rats, for particles fixed *in situ* and in the pellets. Su-13437 treatment results in a 22% average increase in diameter in the tissue and in the pellets from both fractionation procedures. So, if there was breakage of particles during fractionation, it did not affect selectively large peroxisomes.

The fraction of catalase bound to particles depends upon the fractionation procedure used. In Su-13437-treated rats, the pellet from the simplified fractionation contained  $28.5 \pm 2.3\%$  of the enzyme, and the N plus ML fractions of the complete fractionation only  $11.8 \pm 3.0\%$ . The N plus the ML fractions from the control rats also had a significant decrease of particle-bound enzyme (Fig. 21), when compared with the distribution after the simplified fractionation.

This increased solubilization of catalase in control and treated rats, after fractionation with the regular, multiple-step procedure, correlates with

the frequency at which particles showed matrix extraction with formation of ghosts (Table IV). This phenomenon, illustrated in the micrographs of sections through the pellets from both fractionation procedures (Figs. 22–25), affects preferentially the larger peroxisomes with the formation of ghosts or empty particles. The residual matrix adheres to the inner side of the membrane, forming loose clumps. Most extracted particles are in the form of ghosts. Partially extracted peroxisomes, which allowed us to identify the big empty vacuoles as damaged peroxisomes, are not frequent and were seen preferentially in the pellet from control rats (Figs. 22 and 24).

As a general conclusion, we can say that changes in shearing forces induced during homogenization

did not allow the detection of different mechanical properties in proliferated peroxisomes, but these particles were sensitive to the overall fractionation procedure. No morphological evidence of particle breakage during fractionation could be obtained, but the degree of matrix extraction, in normal and treated rats, correlates with the solubilization of catalase. These results suggest that the extracted peroxisomes are responsible for a large fraction of the catalase not bound to particles, in control and Su-13437-treated rats.

#### [<sup>14</sup>C]Leucine Incorporation

The radioactivity incorporated in liver slices, expressed as counts per gram liver in DOC-soluble and immunoprecipitable protein, is shown in Fig.

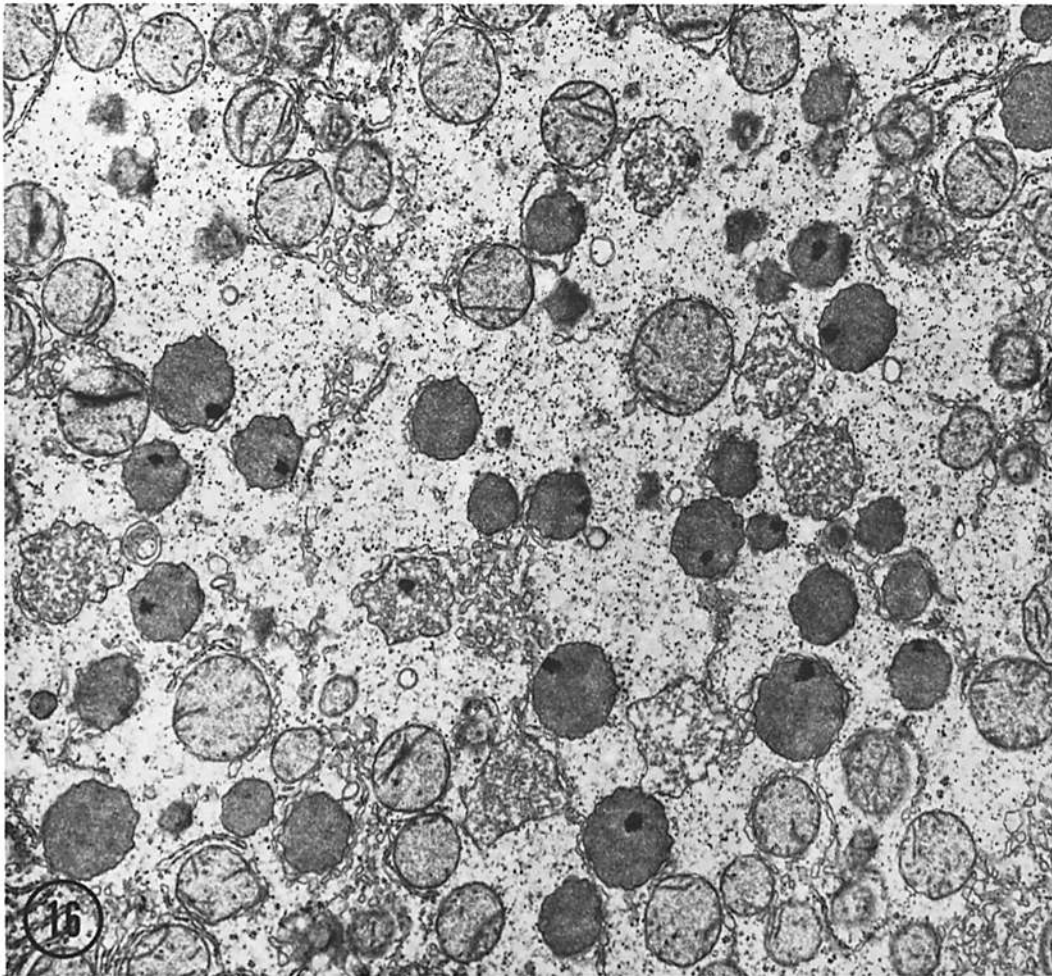


FIGURE 16 Liver structure after 45 days of Su-13437 administration. Peroxisomes are proliferated and have either a normal or a flocculent, low electron density matrix. Nucleoids are present in both types of peroxisomes. A few mitochondria show abnormal aggregation of cristae.  $\times 12,000$ .

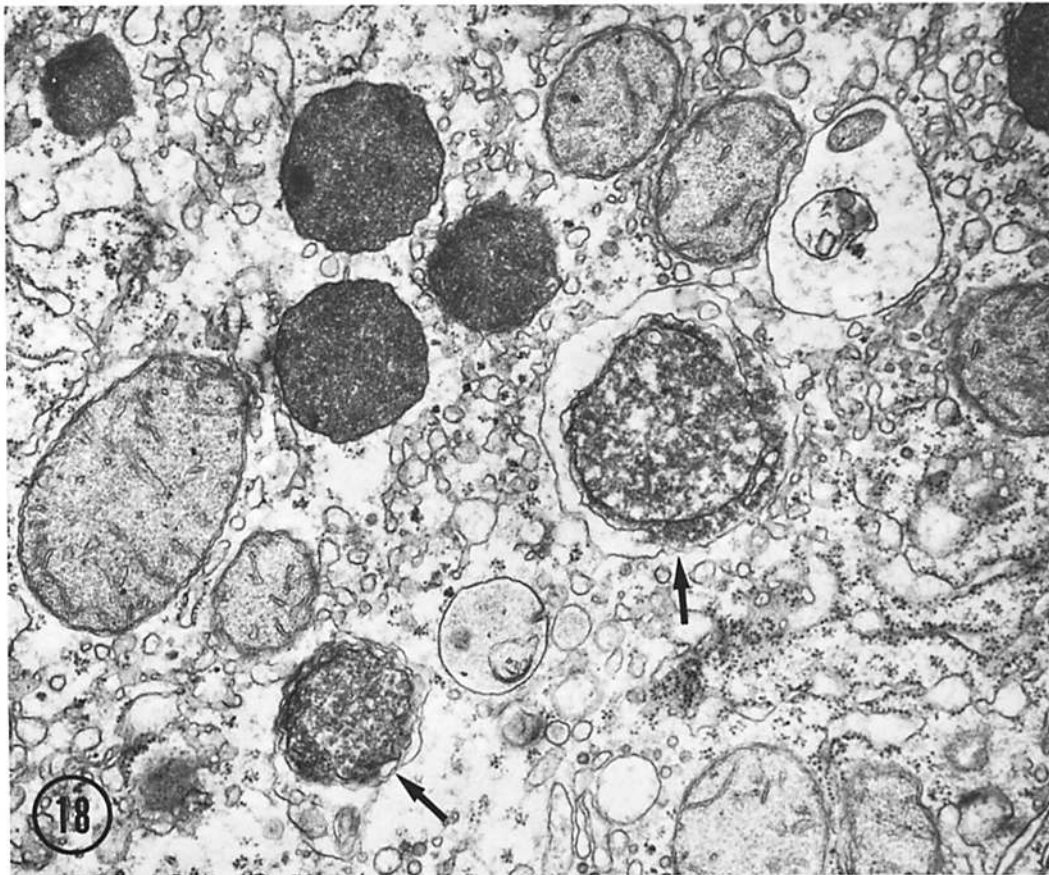
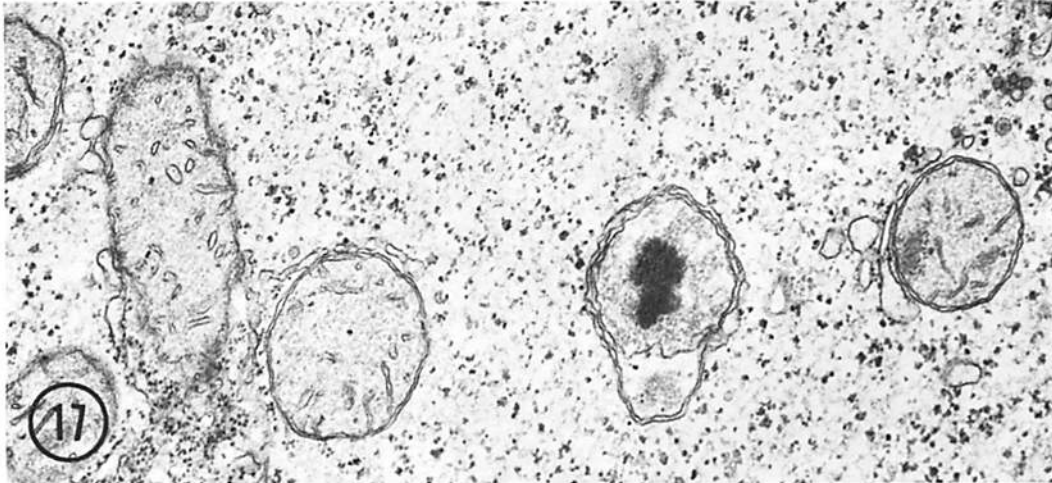


FIGURE 17 Peroxisome-containing autophagosome in control liver. This micrograph illustrates a constant but infrequent finding. The matrix shows signs of disaggregation that are never seen in normal peroxisomes free in the cytoplasm. The background of the micrograph corresponds to an unstained glycogen area.  $\times 24,000$ .

FIGURE 18 Peroxisome-containing autophagosomes in the liver of a rat treated for 3.5 days with Su-13437 (arrows). The peroxisome inside the larger phagosome has already released part of its content. The section also shows several proliferated peroxisomes free in the cytoplasm.  $\times 24,000$ .



26. Maximum incorporation was attained after 1.5 days of treatment, a moment when the rate of liver growth seems to be maximum and yet not much extra tissue mass has accumulated (Fig. 2). Incorporation into antigenic material is doubled, while a lower increment is detected in the DOC-soluble protein.

The effect on antigenic catalase is partially explained by the increase in immunoprecipitate per gram of liver that follows Su-13437 administration: control rats had  $21.5 \pm 1.5$  mg of immunoprecipitate per gram of liver, and  $19.3 \pm 2.2$ ,  $25.4 \pm 0.8$ ,  $25.5 \pm 2.1$ , and  $28.1 \pm 1.7$  after 0.5, 1.5, 3.5, and 6.5 days. These values correspond to an

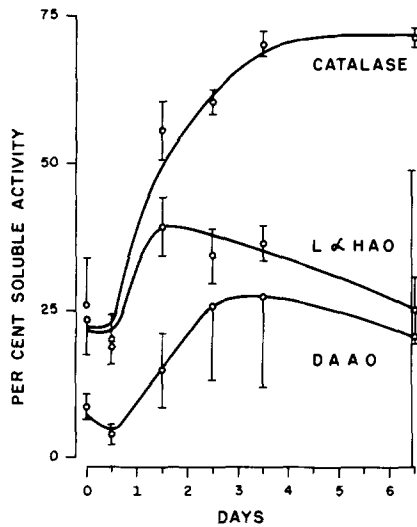


FIGURE 19 Soluble activity of peroxisomal enzymes during Su-13437 administration. Catalase, L-alpha-hydroxy acid oxidase, D-amino acid oxidase, and urate oxidase activities were followed. Urate oxidase was not drawn since it remained always completely bound to particles. Each point corresponds to the average percent fraction of soluble vs. soluble plus particle-bound activities, from four to six rats. To simplify the graph, only one standard deviation bar has been indicated for some points, upwards for catalase and downwards for the oxidases; for the last point of DAAO, the bars are slightly displaced and interrupted. Data derived from single-step fractionations, 10 min at 20,000 rpm in the Sorvall SM-24 rotor.

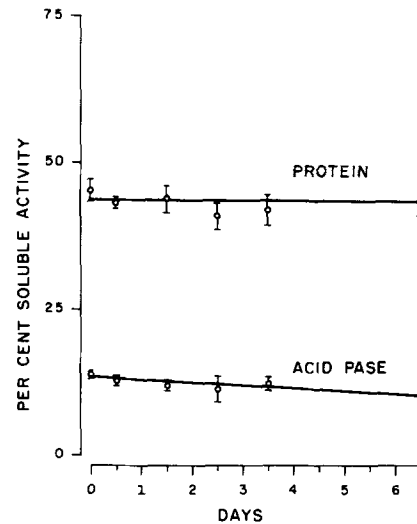


FIGURE 20 Distribution of acid phosphatase and protein during Su-13437 administration. Each point corresponds to the average percent fraction of soluble vs. soluble plus particle-bound activities from four rats. The data derive from single-step fractionations. The slight decrease in percent soluble activity of acid phosphatase is significant:  $0.001 < P < 0.01$  for the significance of  $r$  against zero.

TABLE III  
Release of Particle-Bound Enzymes under Different Homogenization Conditions. Liver from Male Rats Treated for 3.5 Days with Su-13437

Homogenization conditions	Sedimentation in 0.25 M sucrose			Sedimentation in 0.43 M sucrose		
	2 strokes in 0.25 M sucrose	19 strokes in 0.25 M sucrose	<i>P</i> *	2 strokes in 0.25 M sucrose	2 strokes in 1.8 M sucrose	<i>P</i>
	<i>n</i> = 8	<i>n</i> = 4		<i>n</i> = 4	<i>n</i> = 8	
Catalase (control)	$69.5 \pm 5.4$ ‡	$61.3 \pm 3.9$	$<0.025$	$61.0 \pm 0.5$	$36.2 \pm 4.2$	$<0.001$
Catalase (Su-13437)	$30.6 \pm 4.1$	$30.8 \pm 2.9$	$>0.05$	$28.3 \pm 5.0$	$22.9 \pm 4.3$	$>0.05$
Acid phosphatase (control)	$84.7 \pm 2.1$	$83.2 \pm 0.9$	$>0.05$	$83.1 \pm 0.9$	$74.5 \pm 1.8$	$<0.001$
Acid phosphatase (Su-13437)	$87.5 \pm 1.2$	$85.0 \pm 1.7$	$<0.02$	$86.7 \pm 2.0$	$79.3 \pm 1.6$	$<0.001$
Protein (Control)	$54.7 \pm 1.8$	$54.5 \pm 0.8$	$>0.05$	$51.0 \pm 3.3$	$49.2 \pm 2.7$	$>0.05$
Protein (Su-13437)	$54.5 \pm 2.7$	$55.8 \pm 5.8$	$>0.05$	$51.7 \pm 1.6$	$50.9 \pm 1.7$	$>0.05$

\* *P* for the differences calculated applying to Student's *t* test.

‡ Average percent  $\pm$  SD of total activity bound to particles.

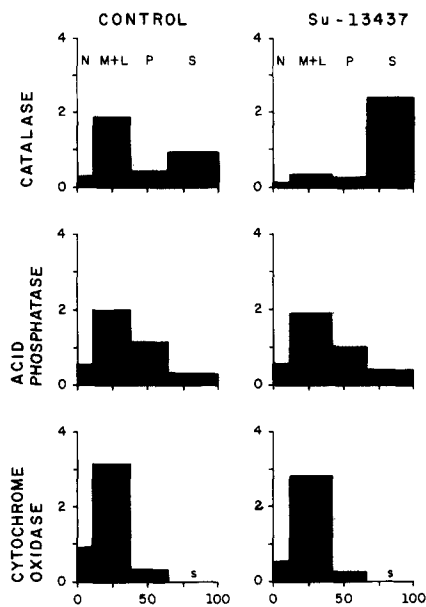


FIGURE 21 Effect of Su-13437 on the subcellular distribution of catalase, acid phosphatase, cytochrome oxidase and protein. Tissue fractionation was carried out according to de Duve et al. (18) by sequential centrifugations and washings at several increasing values of integrated centrifugal force. The abscissa represents cumulative percent protein. The ordinates, percent of enzyme activity over percent of protein, i.e. relative specific activity, for each fraction. The results shown correspond to the average of three fractionations on control rats and four fractionations on rats treated with Su-13437 for 6.5 days. The values for the per cent protein distribution in N, ML, P, and S were  $11.4 \pm 2.2$ ,  $25.8 \pm 2.6$ ,  $26.8 \pm 2.2$ , and  $35.9 \pm 2.4$  for control rats, and  $11.2 \pm 1.1$ ,  $30.8 \pm 2.4$ ,  $24.3 \pm 1.2$ , and  $33.7 \pm 2.3$ , for treated rats. Therefore, a slight increase in the protein content of the ML fraction is detected ( $0.025 < P < 0.050$ ). Acid phosphatase and cytochrome oxidase distributions are not affected by treatment. Catalase, at the new induced levels, shows a marked change in distribution: percent values were  $3.7 \pm 1.9$ ,  $48.9 \pm 12.8$ ,  $12.5 \pm 1.8$ , and  $34.9 \pm 15.2$  for control rats, and  $1.7 \pm 0.5$ ,  $10.1 \pm 2.7$ ,  $7.6 \pm 1.4$ , and  $80.7 \pm 3.5$  for treated rats, in the N, ML, P, and S fractions. The activities of the enzymes and the amount of protein per gram liver were no different from the values found for the other experimental series in this work.

average  $310.2 \pm 52.5 \mu\text{g}$  of precipitated protein per unit catalase activity at all time intervals. DOC-soluble protein levels remained unchanged during the peak of leucine incorporation:  $184 \pm 18 \text{ mg}$  in control rats, and  $165 \pm 8$ ,  $181 \pm 5$ ,  $197 \pm 7$ , and  $207 \pm 7 \text{ mg}$  per gram of liver, after 0.5, 1.5, 3.5, and 6.5 days of treatment. The slight increase

detected by the end of the observation period correlates with the data for total protein. That DOC-soluble protein levels are somewhat higher than those found for the homogenate is attributed to less material being retained during filtration.

The counts per gram of liver incorporated into antigenic material are, for control rats, 0.22% of the counts found in DOC-soluble proteins. When the results are expressed as specific activities, control rats had  $1,375 \pm 189 \text{ cpm per mg DOC-soluble protein}$  and  $26.2 \pm 2.8 \text{ cpm per mg protein}$  of the immunoprecipitate.

These results show that immunoprecipitable catalase increases by 18–30% after Su-13437, and that the apparent change in the rate of synthesis that follows drug administration is higher for the antigenic material than for the average DOC-soluble liver protein.

#### Turnover of Peroxisomal Enzymes

The turnover rates of total and soluble catalase and of D-amino acid oxidase, L-alpha-hydroxy acid oxidase, and urate oxidase were measured according to the procedures detailed in Materials and Methods. The half-lives estimated from the changes in activity after Su-13437, or after AIA for catalase in control and Su-13437 treated rats, have been summarized in Table V. The half-life for total catalase is not affected by the administration of Su-13437. The half-life of induced supernatant catalase, estimated from the kinetics of enzyme accumulation during induction, does not differ from the determinations with total catalase (Fig. 27). The half-lives for the oxidases, calculated from the kinetics of the change in activity to a lower level that for D-amino acid oxidase is practically zero, cannot be differentiated statistically when compared to one another, or with any of the catalase estimations (Fig. 28). The main conclusion derived from these results is that, in treated rats, the soluble catalase and all the peroxisomal enzymes studied have the same half-life with an approximate value of 1.3 days, which is no different from the half-life of catalase in normal rats. In the case of D-amino acid oxidase, its behavior after administration of Su-13437 suggests that its synthesis is blocked by the drug.

#### DISCUSSION

Extending our previous observations (39), we have shown that Su-13437 exerts a marked trophic effect on rat liver peroxisomes. It is more active on

TABLE IV  
*Peroxisome Matrix Extraction after Liver Fractionation*

	Controls	Su-13437	<i>P</i>
	%	%	
Pellet from single step fractionation	53.7 ± 11.0* (53.6)‡	96.7 ± 3.9 (96.1)	<0.001
Pellet from ML fraction	67.8 ± 10.8 (67.1) <i>P</i> < 0.02	100.0 ± 0.0 (100.0) <i>P</i> < 0.02	<0.001

\* Average percentage ± SD. Separate determinations, on an average of 14 micrographs, were made for each group. Each micrograph was considered as a different sample. Calculation of *P* for the effect of treatment, right side column, and for the effect of the fractionation procedure, lower line, was made applying Student's *t* test.

‡ Figures in parenthesis are the effective frequencies, in percent of matrix-extracted sections, derived from all the sections examined. A chi square test applied to the effective frequencies, for the increase in matrix extraction observed in the pellet ML as compared to the pellet from the single-step method, gave a *P* < 0.025 for control rats.

a molar basis than CPIB, another lipid-lowering substance that qualitatively has similar effects on peroxisomes (25, 54, 56, 58). Yet, only Su-13437 is active on peroxisomes of female rats, and the effect we describe on D-amino acid oxidase, equivalent to a complete block of its synthesis, is not shared by CPIB. Differences in the metabolism of these drugs have been found (10) and could explain their properties. Su-13437 also shows a nonspecific effect on liver mass, apparently due to hyperplastic growth; only minor changes in the concentration of various cell components were detected, in contrast with observations on mice (5), where the effect was attributed to both hyperplasia and hypertrophy.

#### *Peroxisome Proliferation*

The volume fraction of liver cells corresponding to peroxisomes increases several-fold after treatment with Su-13437. This effect has not been quantitated by morphometry but is apparent in our morphologic illustrations. Some sections through proliferated peroxisomes are very large, with a diameter of 1.0 μm or more, which is not found in the controls. The 22% average increase in diameter of peroxisome sections does not allow a direct estimate of the increase in the volume of the organelle because of morphometric considerations (4).

The matrix changes in proliferated peroxisomes are remarkable and point again to the change in the properties of the organelle. The forms with decreased electron density of the matrix might correspond to particles being destroyed by atrophy, one of the mechanisms of peroxisome destruc-

tion described by Locke and McMahon in the fat body (44). But low density forms also recall the relation between condensing vacuoles and zymogen granules in the pancreas (32), a resemblance that could be further explored with autoradiography. In rat liver, the normal mechanism of peroxisome degradation is not known, but autophagy is a likely process, judging from the observations on insects (44), and after various experimental conditions (31). Phagosomes with partially degraded peroxisomes, though not frequent, were a constant finding in normal and treated rats.

The nucleoid of peroxisomes appears fragmented initially. As the treatment continues, practically all peroxisomes lack a nucleoid, but the structure is again detectable, with a normal frequency, after several weeks. Occasionally, intact nucleoids were observed in the cytoplasm. Urate oxidase, the only protein identified in the nucleoid, does not lose its activity after *in vitro* solubilization (43) and, further, nucleoids can be reassembled *in vitro* by reprecipitation (F. Leighton, unpublished observations). Apparently, the assembly of urate oxidase as the nucleoid of peroxisomes seems to be affected by Su-13437, since fragmentation, as shown in Fig. 14, was frequently seen at early periods. But soluble fractions, at all time intervals, were systematically negative for urate oxidase activity.

#### *Catalase in the Supernate*

The increase in the soluble fraction of catalase is such that the units of soluble catalase, per gram liver, increase four- to fivefold after treatment. At

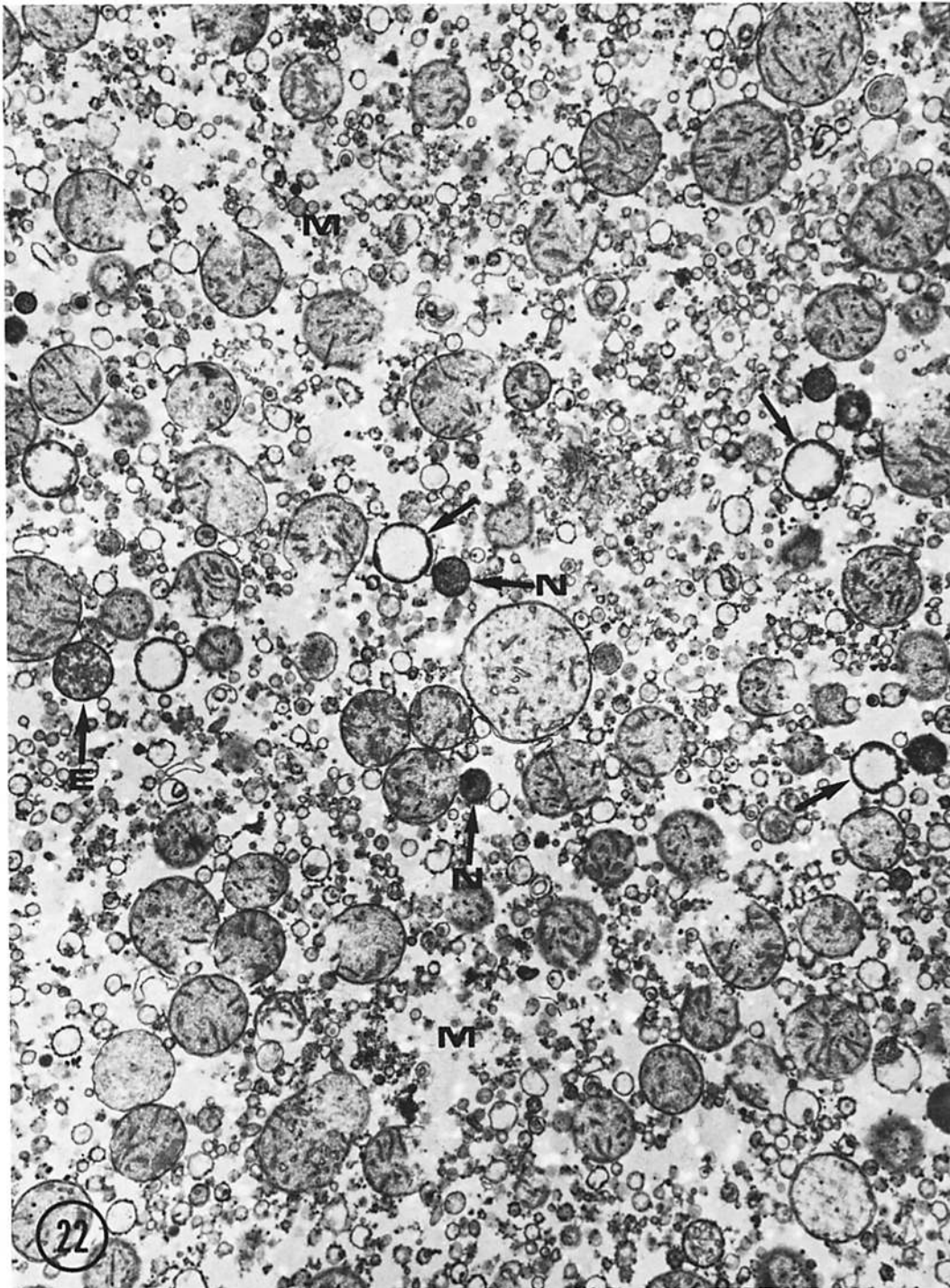


FIGURE 22 Particulate fraction from control liver, prepared by the single-step simplified fractionation procedure. Microsomal vesicles (*M*) are very abundant. There are normal peroxisomes (*N*, arrows), but most of them are affected by matrix extraction with the formation of ghosts (arrows). Partial matrix extraction is occasionally seen (*E* arrow).  $53.7 \pm 11.0\%$  of the peroxisomal profiles were found extracted in micrographs from control rats after this fractionation procedure. The diameter of peroxisomal sections is larger for the extracted forms. An average value of  $0.59 \pm 0.15 \mu\text{m}$ , no different from the diameter of sections in control liver, was found in micrographs of particulate fractions prepared by the single-step method.  $\times 12,000$ .

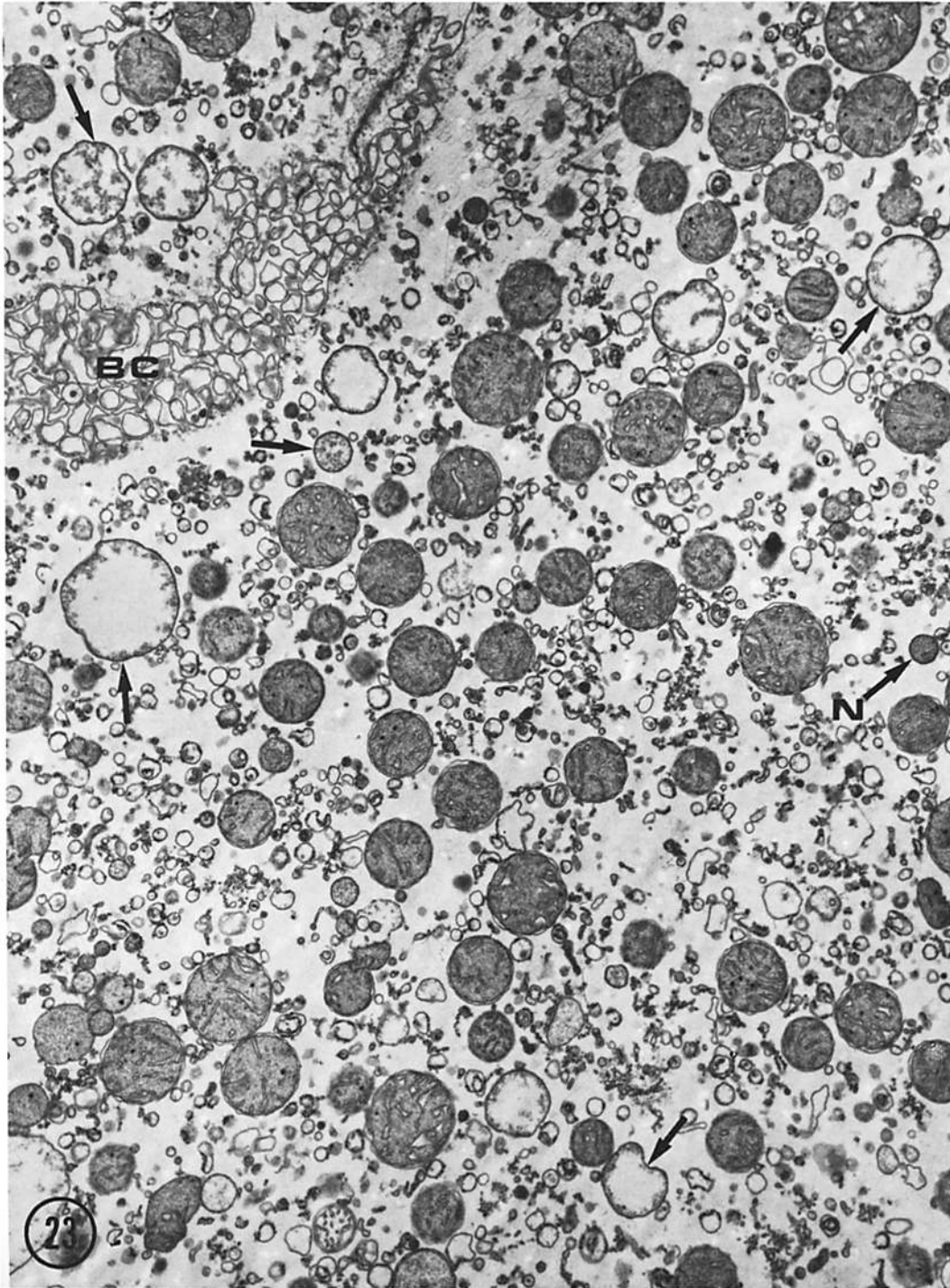


FIGURE 23 Particulate fraction from the liver of a rat treated for 6.5 days with Su-13437, prepared by the single-step simplified fractionation procedure. There is one normal peroxisome (*N* arrow); the rest correspond to extensively extracted particles or ghosts (arrows).  $96.7 \pm 3.9\%$  of peroxisomal sections was found extracted in micrographs from treated rats after this fractionation procedure. The average diameter of peroxisomal sections after treatment, in this and other micrographs, is  $0.69 \pm 0.21 \mu\text{m}$ , no different from the value for proliferated particles fixed *in situ* in the liver. A bile canaliculus (*BC*) illustrates the heterogeneity of this fraction.  $\times 12,000$ .

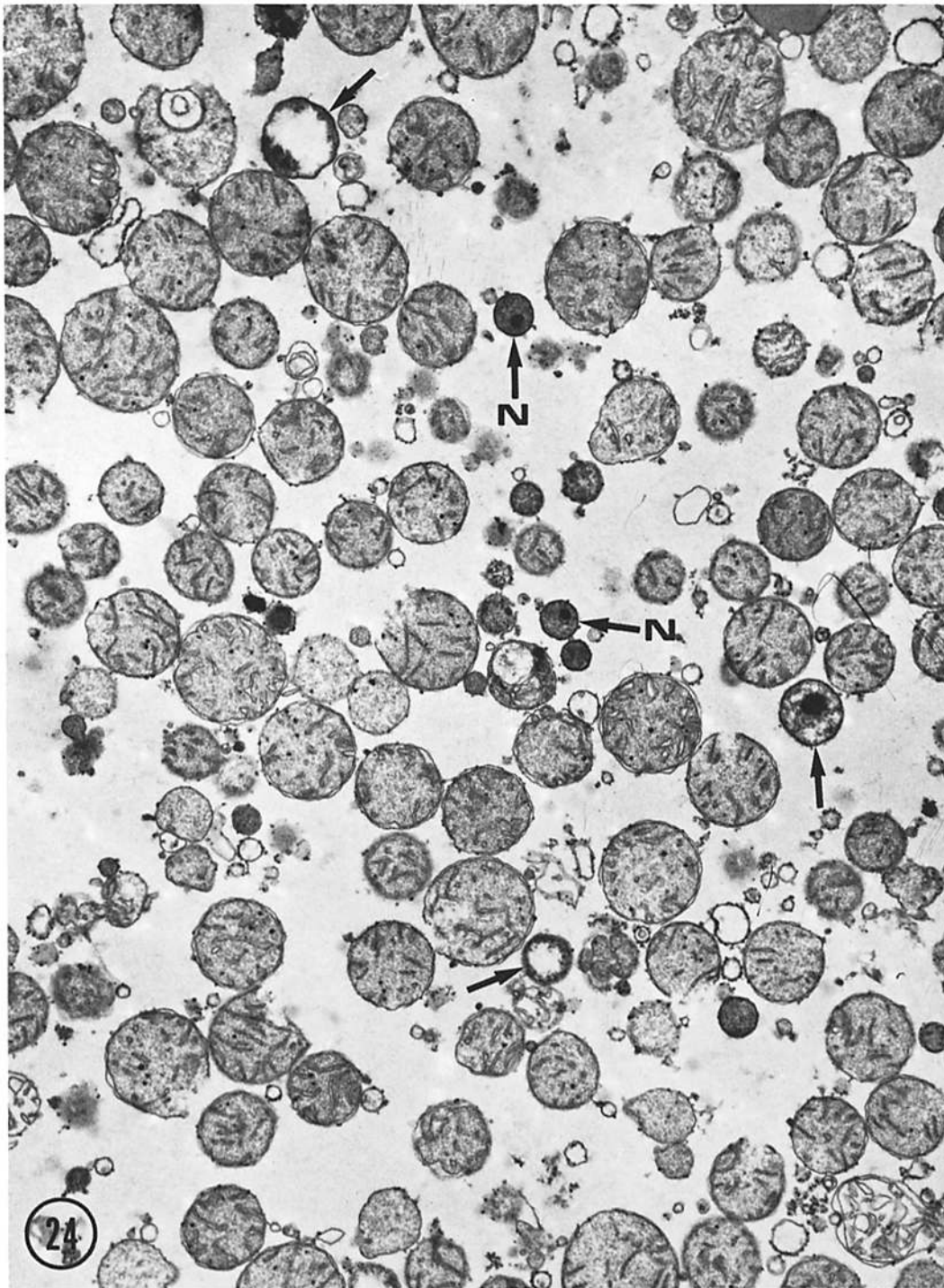


FIGURE 24 ML particulate fraction from a control liver prepared by the multiple-step regular tissue fractionation procedure. Many peroxisome sections (arrows) show partial or complete matrix extraction, a phenomenon found in  $67.8 \pm 10.8\%$  of the peroxisome sections examined in normal rats. The average diameter of these sections was  $0.56 \pm 0.15 \mu\text{m}$ , no different from the average value found for normal particles fixed *in situ* in the liver. Extracted peroxisomes have a continuous membrane and a characteristic submembranous localization of their residual content; they usually correspond to the bigger particles. Normal peroxisomes (*N*) have the same morphological characteristics of normal particles in tissue sections.  $\times 14,000$ .

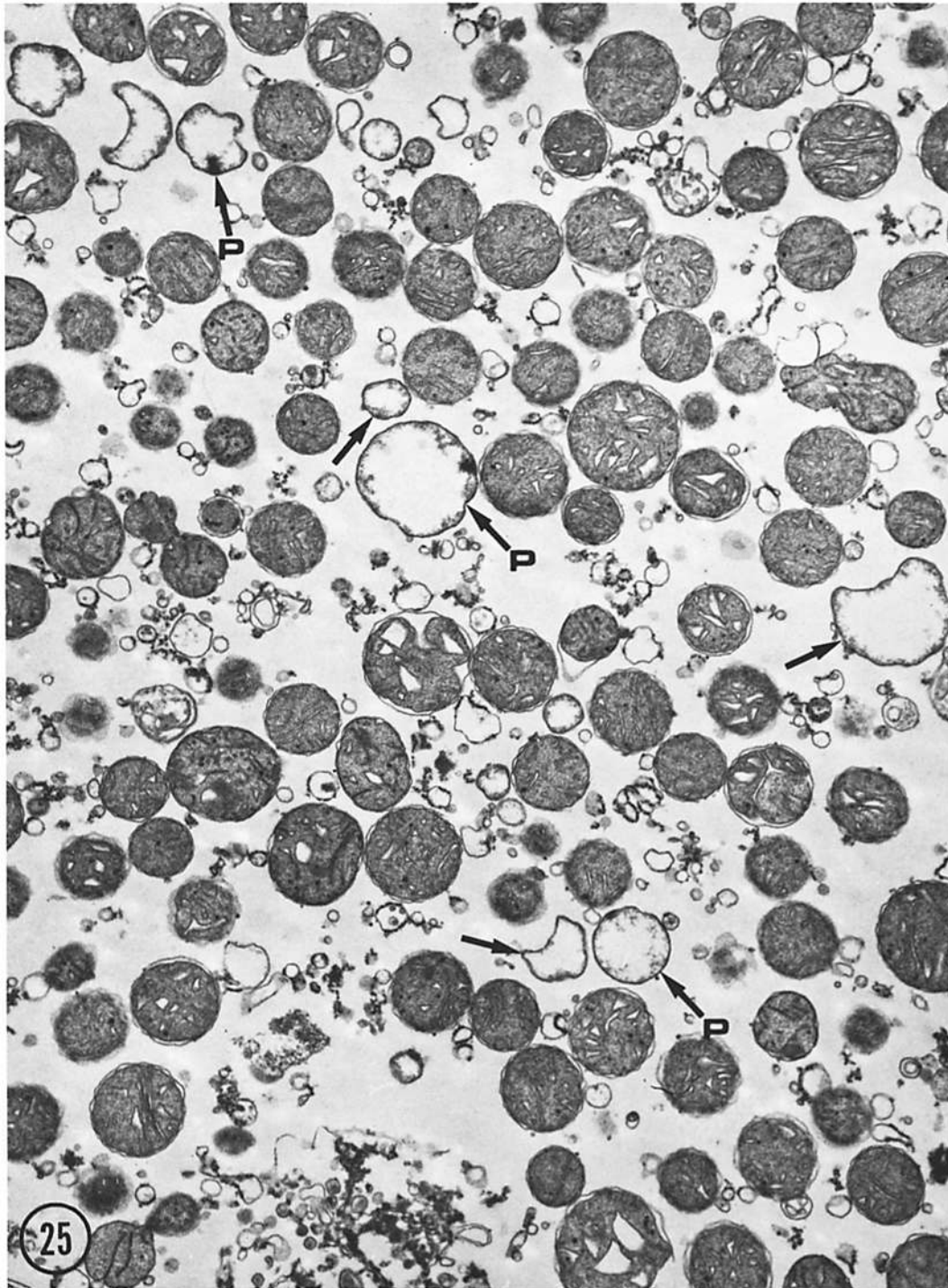


FIGURE 25 ML particulate fraction from the liver of a rat treated for 6.5 days with Su-13437 prepared as the fraction shown in Fig. 24. Only extracted peroxisomes, or ghosts, can be seen (arrows). Normal peroxisomes were never found in ML pellets from treated rats. In some particles (*P* arrows), a clump of electron-dense material, reminiscent of the nucleoid, adheres to the inner side of the membrane. The average diameter of extracted peroxisomes, or ghosts, was found to be  $0.69 \pm 0.18 \mu\text{m}$ , no different from the value for proliferated particles fixed *in situ*, in the liver.  $\times 14,000$ .

the same time, particle-bound catalase per gram liver decreases by one-half.

The origin of the catalase normally present in the supernate has not been established. It could be derived entirely from particles damaged during fractionation (2, 42). According to Lazarow and de Duve (37, 38), the enzyme is assembled inside peroxisomes; moreover, if particle degradation is due to autophagy, the enzyme might never be present in the cell sap. But there are arguments

supporting the idea that, indeed, some of the liver catalase present in the soluble fraction is located in vivo outside peroxisomes.

Several reports on chromatographic and electrophoretic differences between soluble and particle-bound catalases have appeared (20, 27, 28). They can be questioned on the basis that the exposure of the enzyme during fractionation to two different biochemical environments, that of the supernate and that of the particulate fraction, could lead to

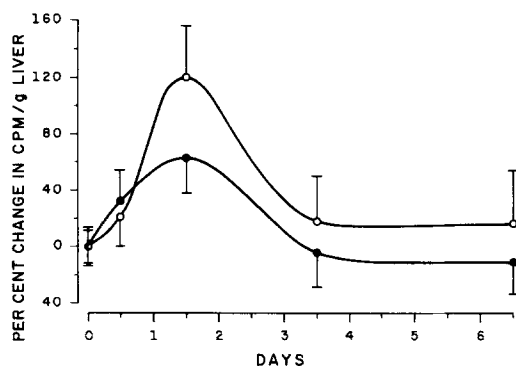


FIGURE 26 [ $^{14}\text{C}$ ]Leucine incorporation into proteins in liver slices from Su-13437-treated rats. Deoxycholate-soluble protein (filled circles). Catalase immunoprecipitate (open circles). Each point is the average of four rats. Results are expressed as the change percent of the cpm per gram liver found in control rats:  $251 \pm 30 \times 10^3$  cpm into DOC-soluble protein and  $563 \pm 77$  cpm into immunoprecipitable catalase. These values correspond to  $1,375 \pm 189$  cpm per mg DOC-soluble protein and  $26.2 \pm 2.8$  cpm per mg protein of the immunoprecipitate. The smaller standard deviation bars at zero time correspond to DOC-soluble protein; for the other points, only one standard deviation, over or below the average point, has been drawn. The relative incorporation increment after 1.5 days is larger for the catalase immunoprecipitate ( $0.025 < P < 0.050$ ).

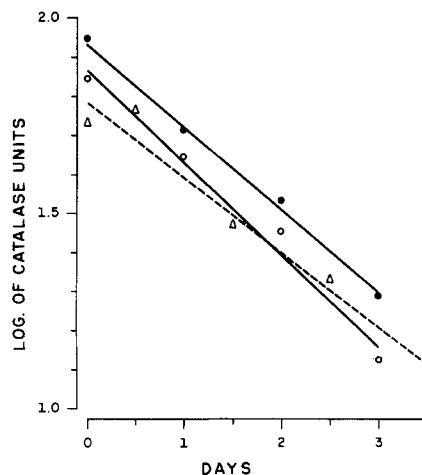


FIGURE 27 Catalase turnover. Semilogarithmic representation of the changes in activity after various treatments: allyl isopropyl acetamide (AIA) was used to block the synthesis of catalase in control rats (open circles), and in rats that had received Su-13437 for 3.5 days (filled circles). The broken line represents turnover of soluble catalase in rats treated with Su-13437. It corresponds to the log of the difference in units with the maximal soluble activity which is the value obtained after 6.5 days. All points are the average of four rats. The half-life values for catalase, calculated from the functions and equivalent to the slope of the lines, are shown in Table V.

TABLE V  
Half-Lives Calculated for Peroxisomal Enzymes and Induced Soluble Catalase

	Half-life	95% confidence interval	<i>n</i> *
	<i>days</i>		
D-Amino acid oxidase	1.25	(1.05-1.53)	30
L-Alpha-hydroxy acid oxidase	1.09	(0.93-1.31)	26
Urate oxidase	1.13	(0.76-2.21)	18
Su-13437-induced soluble catalase	1.56	(1.29-1.97)	20
Total catalase, control, AIA†	1.27	(1.14-1.43)	16
Total catalase, Su-13437, AIA	1.43	(1.23-1.72)	16

\* Number of separate determinations from which the values were derived.

† AIA, allyl isopropyl acetamide.



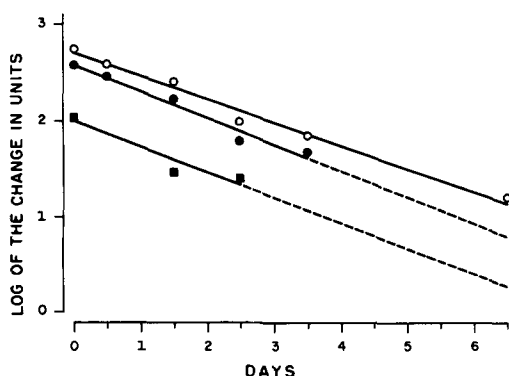


FIGURE 28 Turnover of peroxisomal oxidases during Su-13437 administration. Semilogarithmic representation of the change in activity to a new, lower steady state level reached after 6.5 days. L-alpha-hydroxy acid oxidase (filled circles). Urate oxidase (squares). For D-amino acid oxidase (open circles), the value after 6.5 days was considered to be zero. 10 animals for the control points, and 4 for each determination under treatment. Broken lines are extrapolations to facilitate comparisons. The half-life values calculated from these data are shown in Table V. For the graphic representation, urate oxidase units were multiplied by  $10^2$  and the rest by  $10^3$ .

selective modifications and the artifactual production of two populations. However, by *in vivo* tagging of the catalase molecule with 3-amino-1,2,4-triazole in normal rats, we have found a faster rate of inactivation for the soluble enzyme and a selective increase in the rate of inactivation of the particulate fraction after administration of a peroxisomal oxidase substrate (N. Inestrosa and F. Leighton, unpublished observations). This observation can hardly be explained unless catalase, *in vivo*, is present in two compartments. Our results, as discussed below, are interpreted as indicating that the large increase in soluble activity after Su-13437 corresponds to enzyme released from damaged particles. However, the induction by the drug of a large increase in a normally present nonperoxisomal catalase fraction, accounting for some of the increase in the soluble fraction, cannot be entirely ruled out.

Besides catalase, L-alpha-hydroxy acid oxidase and D-amino acid oxidase distributions are also affected by Su-13437: in all cases, the supernatant fraction is approximately doubled (Fig. 19, Table I). However, the fraction initially present in the supernate is different for each enzyme. If particle breakage with complete release of contents is responsible for supernate activities, all peroxiso-

mal enzymes should be distributed equally. We have shown previously (43) that damage to peroxisomes by freezing and thawing in 0.25 M sucrose is, in fact, followed by a gradual and simultaneous or parallel release of their enzymes. Since this is not the case, some selectivity factor must be involved in their release.

The mechanical resistance of proliferated peroxisomes, under homogenization conditions where the exposure to, or the magnitude of shear forces was greatly increased, was not significantly different from that of the controls. Thus, simple mechanical fragility of the particles does not seem to be the explanation for the soluble fractionation of peroxisomal enzymes. Yet, we show that a normal tissue fractionation procedure, the preparation of an ML fraction which involves repeated centrifugation and resuspension to wash and sediment organelles, will selectively decrease the amount of particle-bound catalase when compared with the single-step fractionation. Since peroxisomes are highly sensitive to hydrostatic pressure damage (12), this factor, rather than the mechanical stress resulting from the resuspension of the pellet during the ML preparation, could explain the extra release of catalase. Proliferated peroxisomes would be even more sensitive to hydrostatic pressure, a hypothesis that can be easily explored. This would account for the fact that the 28.5% of the catalase bound to proliferated peroxisomes decreases to 11.8 when the simplified fractionation procedure is replaced by the complete fractionation. For control rats, the extra release under these conditions is smaller.

The morphological aspect of peroxisomes after fractionation is very different from their appearance when fixed *in situ* in liver cells. Their average diameter does not change, but the matrix is obviously extracted. A fixation artefact, with proteins being removed from a previously damaged particle, might explain the extraction; however, we are inclined to believe that the extraction precedes fixation: the ML fraction from treated rats contains only 5% more liver protein than the controls (Fig. 21). It can be calculated that this extra protein accounts for the increase in cytochrome oxidase and a maximum two- to three-fold increase in peroxisomes, but probably less, since some protein should also be assigned to the additional contamination resulting from proliferated endoplasmic reticulum. Baudhuin et al. (2) have also found a correlation between the extraction of matrix and the release of soluble peroxiso-

mal enzymes to the supernate. In the absence of an accurate morphometric study, a fixation artefact as the explanation of the formation of ghosts cannot be rejected completely. But, on the whole, our results favor the interpretation that cell fractionation procedures damage the particles, causing a partial release of their contents to the soluble fraction and the formation of ghosts or partially emptied peroxisomes.

The difference observed in the proportion of the various peroxisomal enzymes present in the soluble fraction could be attributed to a sieving effect resulting from a differential permeability of the peroxisomal membrane to the organelle enzymes, a situation similar to that found for red blood cells subjected to osmotic stress (46).

The morphologic extraction of peroxisomes that we describe is also present in the organelles prepared by others (2, 14), and should be taken into account when studying the localization of enzymes within peroxisomes from different cell types (11, 30).

The peroxisomal membrane is the most likely target for the postulated fractionation damage leading to extracted peroxisomes. It is known to have peculiar properties that could explain their selective damage. Its lability to hydrostatic pressure has been mentioned; also, it has a high permeability to sucrose (2) and to the substrates of all peroxisomal enzymes (16), a characteristic not shown by other cell membranes.

The apparent permeability to proteins of the peroxisomal membrane leads to the conclusion that isolation of intact proliferated peroxisomes from particulate fractions such as those shown in this work is not possible. In fact, Hess et al. (25) were not able to isolate peroxisomes proliferated after CPIB treatment. They found that the organelles were more labile and equilibrated at lower densities than the controls.

The apparent high permeability of the peroxisomal membrane could explain certain experimental findings and suggests a more complex organization for the particle *in vivo*: isocitric dehydrogenase, NADP linked, was found to be localized in peroxisomes, mitochondria, and the soluble fraction of rat liver (4); perhaps part of the soluble enzyme is, in fact, peroxisomal. Carnitine acyl transferase is another enzyme shown to be partially located in peroxisomes from rat liver (47); it also could be more concentrated in the organelle than the fractionation data allow us to calculate.

### *Turnover of Peroxisomal Enzymes*

The turnover measurements illustrated in Figs. 27 and 28 and summarized in Table V lead to one general conclusion: total liver catalase in control and treated rats, and soluble catalase, D-amino acid oxidase, L-alpha-hydroxy acid oxidase, and urate oxidase from treated rats have a half-life of approximately 1.3 days. It had been previously found (52) that all peroxisomal proteins turn over at the same rate, a result later questioned by Poole (51) after measuring the kinetic parameters of the leucine pool from rat liver. The present findings allow us to reassert the original conclusion, but on a different type of evidence. The conclusion does not agree with the correlation, established by Dehlinger and Schimke (19) and others (60), between the size and the relative rates of degradation of proteins. In fact, we have shown previously, on Sephadex G-200, that the molecular weight of peroxisomal proteins is heterogeneous (43). Thus, our findings are compatible with random degradation of peroxisomes by autophagy.

The equations we have used to measure the turnover have been applied assuming steady state conditions, i.e. that enzyme synthesis equals degradation. In practice this was not so, but we did not introduce corrections because of the difficulties involved in establishing accurately the liver growth function. This simplification is routinely made in turnover studies carried out in growing rats (55). The diluting effect of the increase in tissue mass should result in an underestimation of the real values; still, those values we found for catalase are approximately the same as those calculated for the enzyme with methods that minimize overestimation due to the reutilization of labeled precursors (51, 52).

The half-life observed for the supernate, or soluble catalase according to the complete fractionation, the same as for the rest of the markers, is difficult to interpret. On the whole, it reflects the rate at which the process responsible for the increased levels of catalase appears. Since it is the same as for the other enzyme changes, it seems to be linked to the proliferated peroxisomes and not to a direct or pharmacological effect of the drug on the membranes. The measurement probably represents the turnover rate of the peroxisomal membrane or of its components responsible for the peculiar permeability. This interpretation, based on the hypothesis that the membrane from proliferated particles is more permeable, does not take

into account eventual changes in the surface to volume ratio of the extracted peroxisomes.

Since the half-life of peroxisomal proteins does not change, the proliferation should be the result of an increased rate of synthesis. In fact, a transient but marked increase in the rate of synthesis of catalase was detected upon measuring leucine incorporation into immunoprecipitable catalase. The determinations were made with a crude antiserum, and thus are subject to various artefacts that should be considered: as stated in Materials and Methods, we indirectly discard nonspecific precipitation, since no label was found in the immunoprecipitate of partially hepatectomized rats. From the values we report for protein in the immunoprecipitate, an average  $310 \pm 52 \mu\text{g}$  per unit of catalase, and from what has been found previously with purified catalase and purified antiserum (43), only about one-half of the precipitate can be attributed to catalase. Most of the remaining protein could correspond to catalase precursors without enzymatic activity (37). The relative increments in specific activity for the immunoprecipitable material, and for DOC-soluble proteins, correlate well with the steady state induced levels for catalase and for liver size. In marked contrast to the results for catalase and for the bulk of liver proteins, it can be deduced that the rate of synthesis of the oxidases decreases approximately by 50% and 70% for urate oxidase and L-alpha-hydroxy acid oxidase and by practically 100% for D-amino acid oxidase. This property of Su-13437 also makes it a valuable tool for the study of the biological role of D-amino acid oxidase.

The authors express their gratitude to Mrs. Olivia Walsen and Miss María Nelly Morales for their skillful technical assistance; to Dr. Marcel Bertholds and Dr. Erhold Granzer, Farbwerke Hoechst AG, for supplying Su-13437 and for their interest in this work; and to Dr. Jerome Noble, Ayerst Laboratories, for supplying CPIB. We also thank Drs. Pierre Baudhuin and Miguel Bronfman for valuable suggestions during the preparation of the manuscript.

The revised version of this paper was prepared at the International Institute of Cellular and Molecular Pathology, Brussels, thanks to an invitation extended to Federico Leighton by Dr. Christian de Duve.

This work was supported by grants 47/1969 and 18/1971 of the Comisión Nacional de Investigación Científica y Tecnológica de Chile, and grant 33/1972 of the Fondo de Investigaciones de la Universidad Católica de Chile.

Received for publication 13 February 1974, and in revised form 23 May 1975.

## REFERENCES

1. AUDUS, L. J. 1963. Plant growth substances. Plant science monographs. Interscience Publishers Inc. New York.
2. BAUDHUIN, P., H. BEAUFAY, and C. DE DUVE. 1965. Combined biochemical and morphologic study of particulate fractions from rat liver. Analysis of preparations enriched in lysosomes or in particles containing urate oxidase, D-amino acid oxidase and catalase. *J. Cell Biol.* **26**:219.
3. BAUDHUIN, P., H. BEAUFAY, Y. RAHMAN-LI, O. Z. SELLINGER, R. WATTIAUX, P. JACQUES, and C. DE DUVE. 1964. Tissue fractionation studies. 17. Intracellular distribution of monoamine oxidase, aspartate aminotransferase, alanine aminotransferase, D-amino acid oxidase and catalase in rat liver tissue. *Biochem. J.* **92**:179.
4. BAUDHUIN, P., and J. BERTHET. 1967. Electron microscopic examination of subcellular fractions. II. Quantitative analysis of the mitochondrial population isolated from rat liver. *J. Cell Biol.* **35**:631.
5. BECKETT, R. B., R. WEISS, R. E. STITZEL, and R. J. CENEDELLA. 1972. Studies on the hepatomegaly caused by the hypolipidemic drugs Nafenopin and Clofibrate. *Toxicol. Appl. Pharmacol.* **23**:42.
6. BEEVERS, H. 1969. Glyoxysomes of castor bean endosperm and their relation to gluconeogenesis. *Ann. N. Y. Acad. Sci.* **168**:342.
7. BENNETT, H. S., and J. H. LUFT. 1959. s-Collidine as a basis for buffering fixatives. *J. Biophys. Biochem. Cytol.* **6**:113.
8. BERLIN, C. M., and R. T. SCHIMKE. 1965. Influence of turnover rates on the responses of enzymes to Cortisone. *Mol. Pharmacol.* **1**:149.
9. BEST, M. M., and C. H. DUNCAN. 1970. Lipid effects of a phenolic ether (Su-13437) in the rat: Comparison with CPIB. *Atherosclerosis.* **12**:185.
10. BIANCHINE, J. R., P. WEISS, M. J. T. PEATSON, R. M. HERSEY, and L. LASAGNA. 1970. Metabolism of Su-13437—a new hypolipidemic drug in man. *Clin. Pharmacol. Ther.* **11**:97.
11. BIEGLMAYER, C., J. GRAF, and H. RUIS. 1973. Membranes of glyoxysomes from castor bean endosperm. *Eur. J. Biochem.* **37**:553.
12. BRONFMAN, M., and H. BEAUFAY. 1973. Alteration of subcellular particles induced by compression. *FEBS (Fed. Eur. Biochem. Soc.) Lett.* **36**:163.
13. BURTON, K. 1956. A study of the conditions and mechanism of the diphenylamine reaction for the colorimetric estimation of deoxyribonucleic acid. *Biochem. J.* **62**:315.
14. CHILDS, G. E. 1973. *Hartmanella culbertsoni*: Enzymatic, ultrastructural and cytochemical charac-

- teristics of peroxisomes in a density gradient. *Exp. Parasitol.* **34**:44.
15. DE DUVE, C. 1969. Evolution of the peroxisome. *Ann. N. Y. Acad. Sci.* **168**:369.
  16. DE DUVE, C., and P. BAUDHUIN. 1966. Peroxisomes (microbodies and related particles). *Physiol. Rev.* **46**:323.
  17. DE DUVE, C., J. BERTHET, and H. BEAUFAY. 1959. Gradient centrifugation of cell particles. Theory and applications. *Progr. Biophys. Biophys. Chem.* **9**:325.
  18. DE DUVE, C., B. C. PRESSMAN, R. GIANETTO, R. WATTIAUX, and F. APPELMANS. 1955. Tissue fractionation studies. 6. Intracellular distribution patterns of enzymes in rat liver tissue. *Biochem. J.* **60**:604.
  19. DEHLINGER, P. J., and R. T. SCHIMKE. 1971. Size distribution of membrane proteins of rat liver and their relative rates of degradation. *J. Biol. Chem.* **246**:2574.
  20. FEINSTEIN, R. N., and C. PERAINO. 1970. Separation of soluble and particulate mouse liver catalase by isoelectric focusing. *Biochim. Biophys. Acta.* **214**:230.
  21. FLECK, A., and H. N. MUNRO. 1962. The precision of ultraviolet absorption measurements in the Schmidt-Thannhauser procedure for nucleic acid estimation. *Biochim. Biophys. Acta.* **214**:230.
  22. HAINING, J. L. 1971. On the kinetics of liver enzyme regression following induction. *Arch. Biochem. Biophys.* **144**:204.
  23. HARTMANN, G., and G. FORSTER. 1969. Clinical evaluation of a new hypolipidemic drug, CIBA 13437-Su. *J. Atheroscler. Res.* **10**:235.
  24. HESS, R., and W. L. BENCZE. 1968. Hypolipidaemic properties of a new tetralin derivative (CIBA 13437-Su). *Experientia (Basel)*. **24**:418.
  25. HESS, R., W. STÄUBLI, and W. RIESS. 1965. Nature of the hepatomegalic effect produced by ethylchlorophenoxy-isobutyrate in the rat. *Nature (Lond.)*. **208**:856.
  26. HIGASHI, T., and T. PETERS. 1963. Studies on rat liver catalase. I. Combined immunochemical and enzymatic determination of catalase in liver cell fractions. *J. Biol. Chem.* **238**:3945.
  27. HIGASHI, T., and Y. SHIBATA. 1965. Studies on rat liver catalase. IV. Heterogeneity of mitochondrial and supernatant catalase. *J. Biochem.* **58**:530.
  28. HOLMES, R. S., and C. J. MASTERS. 1969. On the tissue and subcellular distribution of multiple forms of catalase in the rat. *Biochim. Biophys. Acta.* **191**:488.
  29. HUANG, A. H. C., and H. BEEVERS. 1971. Isolation of microbodies from plant tissues. *Plant Physiol.* **48**:637.
  30. HUANG, A. H. C., and H. BEEVERS. 1973. Localization of enzymes within microbodies. *J. Cell Biol.* **58**:379.
  31. HRUBAN, Z., and M. RECHCIGL, JR. 1969. Microbodies and related particles. *Int. Rev. Cytol. Suppl.* **1**.
  32. JAMIESON, J. D., and G. PALADE. 1967. Intracellular transport of secretory proteins in the pancreatic exocrine cell. II. Transport to condensing vacuoles and zymogen granules. *J. Cell Biol.* **34**:597.
  33. KARNOVSKY, M. J. 1965. A formaldehyde-glutaraldehyde fixative of high osmolality for use in electron microscopy. *J. Cell Biol.* **27**(2, Pt. 2):137 a (Abstr.).
  34. KRITCHEVSKY, D. 1971. Newer hypolipidemic agents. *Fed. Proc.* **30**:835.
  35. KRITCHEVSKY, D., and S. A. TEPPER. 1969. Influence of 2-methyl-2-(p-1,2,3,4-tetrahydro-1-naph-tylphenoxy) propionic acid on the oxidation of cholesterol by rat liver mitochondria. *Experientia (Basel)*. **25**:699.
  36. LAMY, J., J. N. LAMY, M. SCHMITT, and J. WEILL. 1973. Effet d'une hépatectomie minimale sur l'activité de la catalase et des oxydases peroxy-somales du foie de rat. *Biochimie (Paris)*. **55**:1491.
  37. LAZAROW, P. B., and C. DE DUVE. 1973. The synthesis and turnover of rat liver peroxisomes. IV. Biochemical pathway of catalase synthesis. *J. Cell Biol.* **59**:491.
  38. LAZAROW, P. B., and C. DE DUVE. 1973. The synthesis and turnover of rat liver peroxisomes. V. Intracellular pathway of catalase synthesis. *J. Cell Biol.* **59**:507.
  39. LEIGHTON, F., and L. COLOMA. 1970. The effect of auxins and related compounds on rat liver. Induction of peroxisomes. *Arch. Biol. Med. Exp.* **7**:R74.
  40. LEIGHTON, F., L. COLOMA, and C. KOENIG. 1971. Inducción de peroxisomas. *Acta Cientifica Venezolana*. **22**(Suppl. 2):R40.
  41. LEIGHTON, F., L. COLOMA, and C. KOENIG. 1973. Recambio de proteínas peroxisomales. *Acta Physiol. Lat. Am.* **23**(Suppl. 3):R186.
  42. LEIGHTON, F., B. POOLE, H. BEAUFAY, P. BAUDHUIN, J. W. COFFEY, S. FOWLER, and C. DE DUVE. 1968. The large-scale separation of peroxisomes, mitochondria, and lysosomes from the livers of rats injected with Triton WR-1339. *J. Cell Biol.* **37**:482.
  43. LEIGHTON, F., B. POOLE, P. B. LAZAROW, and C. DE DUVE. 1969. The synthesis and turnover of rat liver peroxisomes. I. Fractionation of peroxisome proteins. *J. Cell Biol.* **41**:521.
  44. LOCKE, M., and J. T. McMAHON. 1971. The origin and fate of microbodies in the fat body of an insect. *J. Cell Biol.* **48**:61.
  45. LOWRY, O. H., N. J. ROSEBROUGH, A. L. FARR, and R. J. RANDALL. 1951. Protein measurement with the Folin phenol reagent. *J. Biol. Chem.* **193**:265.
  46. MCGREGOR, R. D., and C. A. TOBIAS. 1972. Molec-

- ular sieving of red cell membranes during gradual osmotic hemolysis. *J. Membr. Biol.* **10**:345.
47. MARKWELL, M. A. K., E. J. MCGROARTY, L. L. BIEBER, and N. E. TOLBERT. 1973. The subcellular distribution of carnitine acyltransferases in mammalian liver and kidney. *J. Biol. Chem.* **248**:3426.
  48. MÜLLER, M., J. F. HOGG, and C. DE DUVE. 1968. Distribution of tricarboxylic acid cycle enzymes and glyoxylate cycle enzymes between mitochondria and peroxisomes in *Tetrahymena pyriformis*. *J. Biol. Chem.* **243**:5385.
  49. NEIMS, A. H., D. C. DE LUCA, and L. HELLERMAN. 1966. Studies on crystalline D-amino acid oxidase. III. Substrate specificity and sigma-rho relationship. *Biochemistry.* **5**:203.
  50. NOVIKOFF, A. B., and S. GOLDFISCHER. 1969. Visualization of peroxisomes (microbodies) and mitochondria with Diaminobenzidine. *J. Histochem. Cytochem.* **17**:675.
  51. POOLE, B. 1971. The kinetics of disappearance of labeled leucine from the free leucine pool of rat liver and its effect on the apparent turnover of catalase and other hepatic proteins. *J. Biol. Chem.* **246**:6587.
  52. POOLE, B., F. LEIGHTON, and C. DE DUVE. 1969. The synthesis and turnover of rat liver peroxisomes. II. Turnover of peroxisome proteins. *J. Cell Biol.* **41**:536.
  53. PRICE, V. E., W. R. STERLING, V. A. TARANTOLA, R. W. HARTLEY, JR., and M. RECHCIGL, JR. 1962. The kinetics of catalase synthesis and destruction in vivo. *J. Biol. Chem.* **237**:3468.
  54. REDDY, J. K., D. L. AZARNOFF, D. J. SVOBODA, and J. D. PRASAD. 1974. Nafenopin-induced hepatic microbody (peroxisome) proliferation and catalase synthesis in rats and mice. *J. Cell Biol.* **61**:344.
  55. SCHIMKE, R. T., and D. DOYLE. 1970. Control of enzyme levels in animal tissues. *Annu. Rev. Biochem.* **39**:929.
  56. SVOBODA, D. J., and D. L. AZARNOFF. 1966. Response of hepatic microbodies to a hypolipidemic agent, ethyl chlorophenoxyisobutyrate (CPIB). *J. Cell Biol.* **30**:442.
  57. SVOBODA, D. J., D. AZARNOFF, and J. REDDY. 1969. Microbodies in experimentally altered cells. II. The relationship of microbody proliferation to endocrine glands. *J. Cell Biol.* **40**:734.
  58. SVOBODA, D., H. GRADY, and D. AZARNOFF. 1967. Microbodies in experimentally altered cells. *J. Cell Biol.* **35**:127.
  59. TOLBERT, N. E. 1971. Microbodies—peroxisomes and glyoxysomes. *Annu. Rev. Plant Physiol.* **22**:45.
  60. TWETO, J., P. DEHLINGER, and A. R. LARRABEE. 1972. Relative turnover rates of subunits of rat liver fatty acid synthetase. *Biochem. Biophys. Res. Commun.* **48**:1371.
  61. UMBREIT, W. W., R. H. BURRIS, and J. F. STAUFFER. 1957. *Manometric Techniques*. Burgess Publishing Co. Minneapolis, Minn.
  62. VENABLE, J. H., and R. COGGESHALL. 1965. A simplified lead citrate stain for use in electron microscopy. *J. Cell Biol.* **25**:407.